The Vaca Muerta transgression (Upper Jurassic), Neuquén Basin, Argentina: Insights into the evolution and timing of aeolian–marine transitions

Maximiliano Paz[1], Juan José Ponce[2,3,4] , M. Gabriela Mángano[1], Noelia Beatriz Carmona[5,6], Andreas Wetzel[7], Egberto Pereira[8], Maximiliano Nicolás Rodríguez[5,6]

[1] Department of Geological Sciences, University of Saskatchewan, 114 Science Place, Saskatoon, SK, S7N 5E2, Canada
[2] Consejo Nacional de Investigaciones Científicas y Técnicas (CONICET), Argentina
[3] Servicio Geológico Minero Argentino (SEGEMAR), Centro General Roca, Río Negro, SEGEMAR Regional Sur, Independencia 1495. Parque Industrial 1, General Roca, Río Negro, Argentina
[4] Universidad Nacional de Río Negro (UNRN), Argentina
[5] Instituto de Investigación en Paleobiología y Geología, Universidad Nacional de Río Negro, General Roca, Río Negro, 8332, Argentina
[6] Instituto de Investigación en Paleobiología y Geología (IIPG), CONICET, Av. J. A. Roca 1242, General Roca, Río Negro, 8332, Argentina
[7] Departement Umweltwissenschaften – Geologie, Universität Basel, Bernoullistrasse 32, Basel, CH-4056, Switzerland
[8] Faculdade de Geologia – Departamento de Estratigrafia e Paleontologia, Universidade do Estado do Rio de Janeiro, Bloco A – Sala 2020, Rua São Francisco Xavier 524, Maracaña, Rio de Janeiro, 20559-900, Brasil

Published 2021 in: Sedimentology, 68: 2732–2764 (26 March 2021) doi:10.1111/sed.12872

Abstract

Considering the evolution of aeolian to marine transitions for the geological record, either catastrophic or gradual transgressive scenarios showing high or low rates of coastal migration have been proposed. A critical evaluation of modern analogues suggests that a catastrophic transgression shares many characteristics with Holocene transgressions, yet they are caused by different rates of sea-level rise. The present study provides insights into the evolution of aeolian to marine transitions in order to discuss these alternative scenarios of sea-level rise. For this purpose, a sedimentological and ichnological analysis was carried out on ten stratigraphic sections of the Picún Leufú area, Argentina. There, marine deposits of the Vaca Muerta Formation accumulated over the aeolian deposits of the Quebrada del Sapo Formation during the early Tithonian. The sedimentary evolution of the transition can be summarized in: (i) a shutdown of aeolian dune field deposition, generating a planation surface in somewhat elevated areas and reworked megadunes in lowlands; (ii) beach sedimentation caused by episodic marine flooding that contributed to megadune reworking; and (iii) deposition in an embayed marginal-marine setting at the coast, recorded by bay margin bindstone, proximal bay and distal bay sedimentation. This transition indicates very rapid coastline migration and a condensed Transgressive Systems Tract succession throughout the study area. Rates of sea-level rise similar to Holocene ones (millimetres to centimetres per year) may have produced the transition between the Quebrada del Sapo and Vaca Muerta formations. The Late Jurassic represents a non-glacial time, and the global sea-level maximum highstand pre-dated the Vaca Muerta transgressive event. Thus, part of the sea-level rise has to be attributed to tectonic/thermal subsidence and compaction of underlying strata, which may have generated these atypical rapid rates of sea-level rise.

INTRODUCTION

During transgressions, a relative sea-level rise fosters landward migration of facies and sediment reworking through ravinement erosion, as well as sediment storage within marginal-marine environments and a decrease in sediment transfer towards the basin centre (Swift, 1968; Nummedal & Swift, 1987; Cattaneo & Steel, 2003). Shoreline trajectories can record sediment thickness variations depending on the coastal gradient (Cattaneo & Steel, 2003). While thick successions occur in incised valleys (Belknap & Kraft, 1981), transgressive deposits are thinner, have a lower preservation potential, and represent a telescopic record of sea-level rise in interfluve areas (e.g. Joeckel & Korus, 2012). When a transgression takes place over a dune field, aeolian bedforms can be reworked in different ways and stratigraphic hydrocarbon traps form in many cases (e.g. van West, 1972; Vincelette & Chittum, 1981; Moore, 1983; Desmond *et al.,* 1984; Fryberger, 1984). Flooding of dune fields results in an 'inherited', 'reworked' or 'erosional' relief or a planation surface, depending on the amount of reworking (Fryberger, 1986; Eschner & Kocurek, 1988). This is controlled by several factors, such as aeolian-dune sand-budget, dune orientation with respect to the coast, prevailing wind direction, marine processes, precipitation and rate of relative sea-level rise (Eschner & Kocurek, 1988).

At present, ancient examples of aeolian to marine transitions are explained using either gradual transgressions occurring in the range of Myr and represented by several parasequences showing a retrogradational stacking pattern (Jordan & Mountney, 2012), or invoking catastrophic rates of sea-level rise (metres per day; Garcia-Castellanos *et al.,* 2009) that generate limited transgressive successions (Ahmed Benan & Kocurek, 2000), such as the abrupt flooding of the Mediterranean Sea (Blanc, 2002; Abril & Periáñez, 2016). This study presents an alternative model where a transgression over an aeolian dune field can be constituted by a thin retrogradational succession that may have been deposited following Holocene rates of sea-level rise (millimetres to centimetres per year; Hanebuth *et al.,* 2000).

The Picún Leufú area in Argentina (Fig. 1), offers exceptional outcrops exposing the transgression of the Upper Jurassic–Lower Cretaceous Vaca Muerta Formation over the Kimmeridgian Quebrada del Sapo Formation (lateral equivalent of the Tordillo Formation). The aims of this study are to: (i) describe and interpret the sedimentary facies of the transgressive succession of the Vaca Muerta Formation; (ii) decipher the processes and factors that affected its development; (iii) critically evaluate previous hypotheses about the flooding of modern and ancient aeolian dune fields; and (iv) discuss a classification scheme comprising gradual, rapid and catastrophic transgressions over aeolian successions.

GEOLOGICAL SETTING

The Neuquén Basin is located in western-central Argentina, bounded by cratonic areas at its north-east and south-east margins, and by the Andean magmatic arc to the west (Fig. 1). The basin contains about 7000 m thick sediments deposited from Late Triassic–Early Jurassic to Cretaceous times (Fig. 2; Arregui et al., 2011). The development of the basin is commonly subdivided into three major stages according to the tectonic setting, namely syn-rift, back-arc (post-rift) and foreland stage (Howell et al., 2005). Upper Triassic–Lower Jurassic volcaniclastic and siliciclastic continental deposits constitute the syn-rift stage, grouped into the Precuyano Cycle (Gulisano, 1981; Carbone et al., 2011). During the Early Jurassic, a magmatic arc formed along the western margin of Gondwana and a back-arc basin developed within the continent due to the onset of subduction (Mpodozis & Ramos, 2008). Since this time and until the Early Cretaceous, marine and continental sedimentation alternated in response to sea-level fluctuations, subsidence and deposition, as recorded by the Cuyo, Lotena and Mendoza groups.

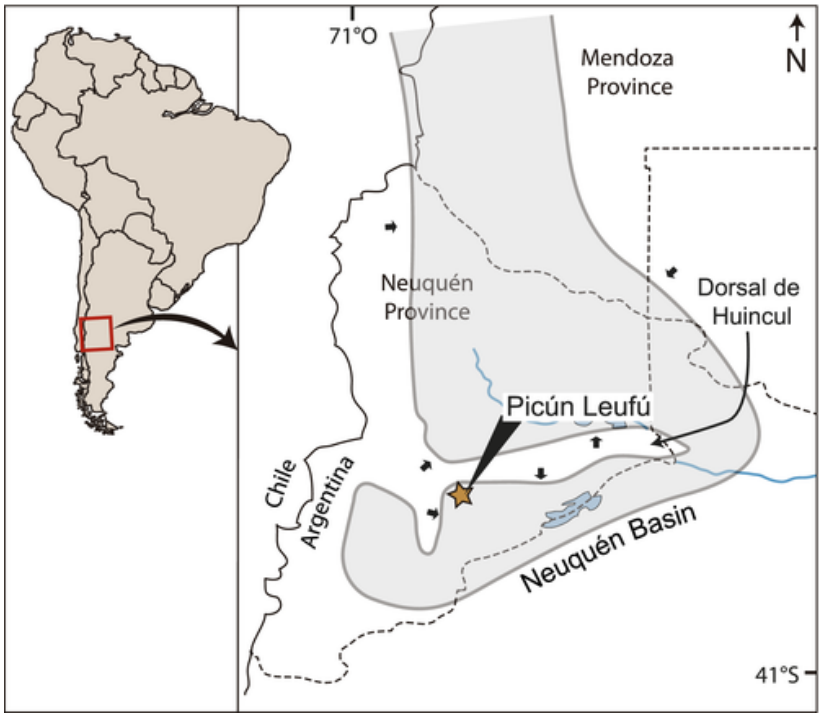

Fig. 1 Location of the study area. Left – South America, red frame represents detailed map shown to the right. Right – Study area marked by orange asterisk in the Kimmeridgian palaeo-geographic reconstruction of the Neuquén Basin (grey shaded). Black arrows show sediment source areas. Modified from Vergani *et al*. (1995).

During the Late Cretaceous, a compressional tectonic regime led to the closure of the connection with the Pacific Ocean, and the Neuquén Basin entered a foreland basin stage (Ramos & Folguera, 2005; Tunik *et al.,* 2010).

The Vaca Muerta Formation comprises upper lower Tithonian to lower Valanginian marine deposits of the Mendoza Group (Stipanicic *et al.,* 1968). The Vaca Muerta Formation belongs to the Lower Mendoza Mesosequence (Fig. 2; Legarreta & Gulisano, 1989), a sequence-stratigraphic entity bound at the base and top by the intra-Upper Jurassic and the intra-Valanginian unconformity, respectively. This mesosequence starts with the continental deposits of the Tordillo Formation and their lateral equivalents (for example, Quebrada del Sapo Formation), which are covered by marine deposits of the Vaca Muerta Formation. The transgression approached from the Pacific Ocean due to a relative sea-level rise (Leanza *et al.,* 2011). At the top, the Vaca Muerta Formation shows a transitional and diachronous contact with the overlaying nearshore deposits of the Quintuco Formation and its lateral equivalents (Legarreta & Gulisano, 1989). The Vaca Muerta Formation is composed of mudstone, marl and limestone that are commonly referred to as black shales due to their high organic matter content [on average 3 to 8% total organic carbon (TOC) and peak values of 10 to 12%; Uliana *et al.,* 1999].

The transgression of the Upper Jurassic–Lower Cretaceous marine Vaca Muerta Formation over the Upper Jurassic continental Tordillo Formation constitutes an excellent example of an aeolian–marine transition that has been recurrently studied (Mutti *et al.,* 1994; Boll & Valencio, 1996; Cevallos, 2005; Borbolla *et al.,* 2014; Ponce *et al.,* 2015, 2016). Contrasting hypotheses concerning the transgression were proposed. Originally, the shift from the Tordillo to the Vaca Muerta formations was seen as transitional, resulting in a conformable contact (e.g. Leanza *et al*., 1977; Zanettini, 1979). Later, Mutti *et al*. (1994) and Legarreta (2001, 2002) emphasized the abrupt shift from continental Lowstand Systems Tract (LST) dune facies to marine conditions during the Transgressive Systems Tract (TST). Consequently, the transition from the Tordillo to the Vaca Muerta formations was suggested to represent a Jurassic equivalent to the sudden flooding of the Mediterranean Sea during Zanclean times at the end of the Messinian Salinity Crisis (Mutti *et al.,* 1994). In contrast, based on seismic, well log and outcrop informa-

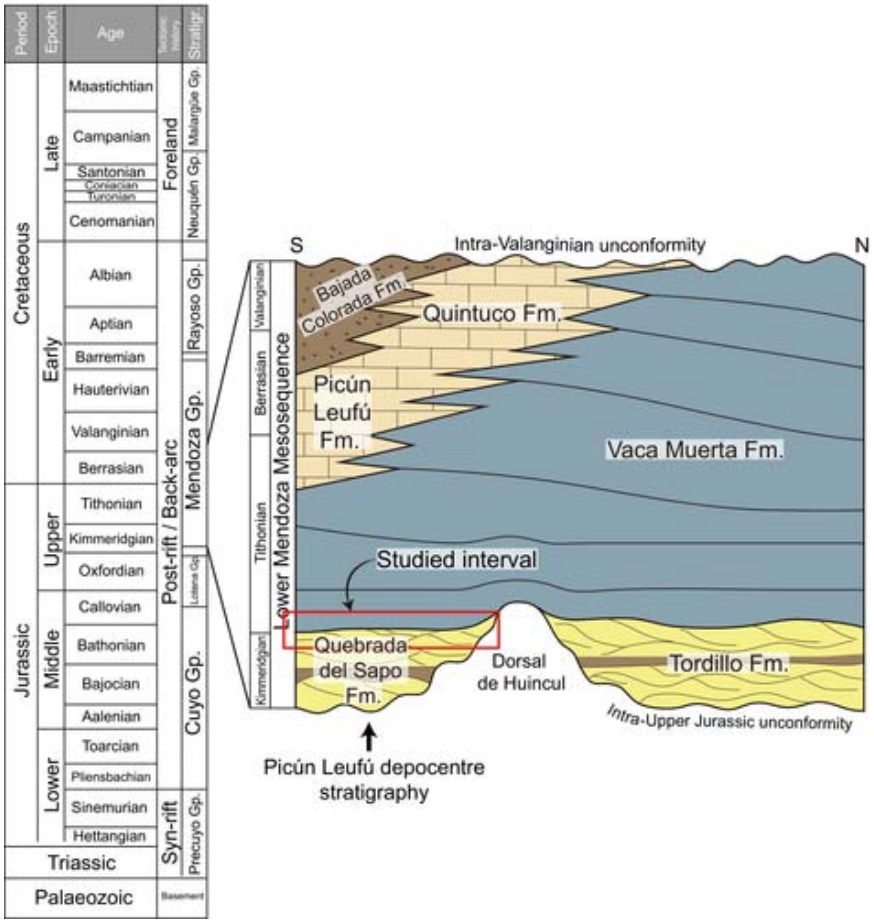

Fig. 2 Stratigraphy of the Neuquén Basin, fourth column from the left indicates tectonic stages of the Neuquén Basin. To the right a south–north section of the Lower Mendoza Mesosequence in the Picún Leufú area, traversing the Dorsal de Huincul (modified from Howell *et al.*, 2005); the studied interval is marked by a red frame.

tion, Boll & Valencio (1996) proposed a transgression characterized by a basal transgressive deposit above an erosive unconformity that truncates the Tordillo Formation. Later, Cevallos (2005) recognized a partly inherited to partly reworked aeolian megadune's relief in plan-view seismic records on top of the Catriel Formation (lateral equivalent of the Tordillo Formation), and argued in favour of a catastrophic transgression. In this case, the transgression was seen in terms of its timing to represent an equivalent to the Holocene flooding of the Black Sea (Ryan & Pitman, 1998). Since then, a catastrophic flooding has been the widely accepted hypothesis for the transgression of the Vaca Muerta Formation (Leanza *et al.*, 2011).

Picún Leufú anticline and Quebrada del Sapo domain

The study area is located near the intersection between the Picún Leufú creek and National Route 40. It comprises the north-western part of the Picún Leufú depocentre and the westernmost edge of the Dorsal de Huincul ridge system (Fig. 1), in particular, the south-verging, east–west trending Picún Leufú anticline. The study area can be differentiated in the Picún Leufú domain (PL, sections 1 to 4) and an area associated with a NNE-oriented ravine, known as Quebrada del Sapo (QdS, sections 5 to 10, Fig. 3).

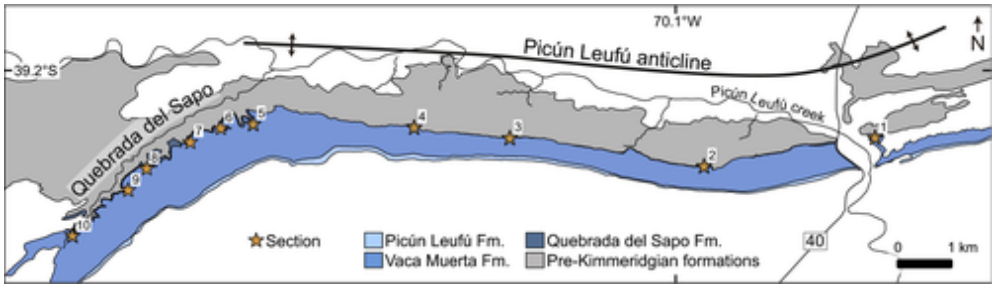

Fig. 3 Map of the study area showing the location of sections.

In the study area, the Lower Mendoza Mesosequence is represented by the Quebrada del Sapo, Vaca Muerta and Picún Leufú formations (Fig. 2). The Quebrada del Sapo Formation (Parker, 1965; Digregorio, 1972) is Kimmeridgian in age as evidenced by lithostratigraphic correlation with the Tordillo Formation (Veiga & Spalletti, 2007). However, a supposed unconformity between these two units may indicate a slightly younger age for the Quebrada del Sapo Formation (Zavala *et al.,* 2008). The latter is composed of conglomerate, sandstone and mudstone deposited in fluvio-lacustrine, fluvial and aeolian settings (Zavala *et al.,* 2005; Spalletti & Veiga, 2007; Veiga & Spalletti, 2007). The aeolian facies covers an extensive area and, hence, it was interpreted as recording a dune field (Zavala *et al.,* 2005). A sharp to erosive surface separates the Vaca Muerta Formation above from the Quebrada del Sapo Formation below (see Ponce *et al.,* 2015, 2016, for details).

The Vaca Muerta Formation comprises up to *ca* 350 m of marine siliciclastic and carbonate deposits in the study area. At the top, the Picún Leufú Formation overlays the Vaca Muerta Formation by a gradational contact. The latter formation consists of shallow-marine sandstone, mudstone and limestone, reflecting an overall upward increase in carbonate content. Correlation based on ammonite biostratigraphy shows an early Tithonian to early Berrasian age for both formations (Leanza & Hugo, 1977). Several sedimentological and sequence stratigraphic studies agree that the Vaca Muerta and Picún Leufú formations record a mixed carbonate–siliciclastic system (Leanza, 1973; Spalletti *et al.,* 2000; Freije *et al.,* 2002; Zavala & Freije, 2002; Zeller, 2013; Zeller *et al.,* 2015; Krim *et al.,* 2017, 2019; Paz *et al.,* 2019). In this area, most of these sedimentological studies have dealt with the basal TST and envisaged a catastrophic transgression, yet they did not address the transgressive deposits from an integrated sedimentological and ichnological perspective.

Early Jurassic to Early Cretaceous syn-sedimentary tectonics in the Dorsal de Huincul area played a major role for the development and configuration of facies and sediment source areas. Stratal geometry and associated unconformities of the Picún Leufú anticline record successive pulses of growth (Freije *et al.,* 2002; Zavala & Freije, 2002; Naipauer *et al.,* 2012). During the Kimmeridgian to middle Tithonian (lower *Aulacosphinctes proximus* ammonite zone of Parent *et al.,* 2011), syn-sedimentary deformation affected the Lower Mendoza Mesosequence in the anticline, whereas in the QdS domain the strata are almost undeformed. Tectonic movements caused progressive development of unconformities and normal faults within the Mendoza Mesosequence. An upward gradually decreasing dip of the Quebrada del Sapo Formation and the lowermost *ca* 100 m of the Vaca Muerta Formation record waning deformation that ends with subhorizontal strata of the middle and upper Vaca Muerta and Picún Leufú formations. The progressive unconformities are represented by a change in dip between the Lotena and Quebrada del Sapo formations (30°), the fluvial and aeolian unit of the Quebrada del Sapo Formation (9°), the Quebrada del Sapo and Vaca Muerta formations (2 to 17°), and above the first 80 to 120 m of the Vaca Muerta Formation (10 to 23°). Syn-sedimentary normal faults cross-cut the uppermost part of the Quebrada del Sapo Formation dune deposits and up to *ca* 50 m of the lowermost Vaca Muerta Formation. A post-depositional deformational episode generated an additional *ca* 30° tilt of the whole succession, showing its maximum to the east of the anticline and a decrease towards the west (QdS).

METHODS

The Picún Leufú area shows exceptional outcrops of the Quebrada del Sapo and Vaca Muerta formations, 12 km long in the east to west direction at PL and 5.5 km long in the north-east/south-west direction at QdS, that were suitable for logging sedimentary sections. The main analysis is focused on the aeolian–marine transition represented by the uppermost 0.5 to 2.0 m

of the Quebrada del Sapo Formation and the lowermost 3 to 25 m of the Vaca Muerta Formation. Dip angle and azimuth were measured with a clinometer and compass to assess the tectonic deformation of the succession. A short description of the Quebrada del Sapo Formation continental deposits is provided, in order to unravel the pre-flooding topography and determine its associated sedimentary environments based on previous studies in the area (Zavala *et al.*, 2005; Spalletti & Veiga, 2007; Veiga & Spalletti, 2007). In contrast, the Vaca Muerta Formation facies are numbered because of a higher detail of analysis.

Sedimentological and ichnological analyses of the top of the Quebrada del Sapo Formation and the Vaca Muerta Formation transgressive succession were carried out while logging ten sections on a bed by bed scale (Fig. 3), four sections in PL and six sections in QdS. The lithology, sedimentary structures, trace fossil and body fossil content of each facies have been recorded. Lithofacies classification was used as a descriptive term to subdivide rocks showing different sedimentological aspects within a facies. Facies comprises sedimentary features and related processes in a specific subenvironment of deposition. Facies association was used to describe a group of facies occurring in a depositional environment. Petrological observations were made on thin sections of seven samples from the Vaca Muerta Formation. The ichnological analyses comprise the description of ichnotaxa and estimation of the degree of bioturbation that is expressed as bioturbation index (BI) as proposed by Taylor & Goldring (1993), ranging from unbioturbated (BI = 0) to completely bioturbated (BI = 6). Mudstones are classified following Lazar *et al*. (2015). The sequence stratigraphic interpretation was based on facies stacking pattern and interpretation of stratigraphic surfaces, following the nomenclature of Catuneanu (2006).

SEDIMENTARY FACIES

Quebrada del Sapo Formation: Fluvial facies association

Sandy conglomerate and pebbly sandstone facies

Description. This facies consists of thin to thick-bedded, clast or matrix-supported sandy conglomerate, pebbly sandstone and medium to coarse-grained sandstone (Fig. 4). The conglomerate and sandstone display normal grading, trough cross-bedding, low-angle cross-bedding, horizontal bedding and subordinate current ripples in the sandstone. The conglomerate is polymictic and consists of rounded cobbles to granules of predominantly volcanic and plutonic origin. The gravelly sandstone is medium to coarse-grained with a minor content of cobbles and pebbles. The conglomerate occurs in lenticular-shaped, amalgamated, 10 to 50 cm thick, stacked packages that commonly have a slightly convex, erosive base. Sandstone beds are 20 to 100 cm thick and commonly encase conglomerate. The complete facies forms 3 to 21 m thick intervals, and rests on red mudstone facies or trough cross-stratified sandstone facies (see below).

Fig. 4 Facies of the Quebrada del Sapo Formation. (A) Panoramic view close to section 7 showing the fluvial and aeolian facies association (Fluvial FA and Aeolian FA) and the overlying Vaca Muerta Formation. (B) Fluvial facies association in outcrop showing trough cross-bedded conglomerates overlain by red and green lacustrine mudstone. (C) Large-scale trough cross-bedded sandstone of the aeolian facies association (people for scale are *ca* 1.7 m tall).

Interpretation. The trough cross-bedded deposits were formed by migration of three-dimensional dunes, whereas the low-angle cross-bedded and horizontal-bedded deposits represent migration of low-relief sediment waves (Paola *et al.,* 1989). The stacking of conglomerate within lenticular-shaped bodies suggests bedform migration in fluvial channels, constituting channel-bar deposits. Zavala *et al*. (2005) interpreted these facies as dense flows of fluvial origin. Veiga & Spalletti (2007) differentiated between lenticular bodies representing the accumulation of in-channel and marginal bars and minor channel fills, and sheet-like geometries comprising short-lived, high-energy sheetfloods.

Red to green mudstone facies

Description. This facies is represented by 1 to 15 m thick successions of red to green massive mudstone. The facies is interbedded with sandy conglomerate and pebbly sandstone facies.

Interpretation. In the study area, these fine-grained deposits associated with sandstone and conglomerate facies were interpreted as lacustrine because of lacking evidence for subaerial exposure (Zavala *et al.,* 2005), or as deposited on an ephemerally flooded mudplain due to their association with fluvial facies (Veiga & Spalletti, 2007). The latter authors suggested that the massive appearance of the mudstone can be related to bioturbation and incipient pedogenesis (Veiga & Spalletti, 2007).

Matrix-supported pebble to cobble conglomerate facies

Description. This facies comprises 5 to 10 cm thick, matrix-supported, structureless pebble to cobble conglomerate. It occurs locally at the top of sandy conglomerate facies, towards the transition to the Vaca Muerta Formation.

Interpretation. This facies represents fluvial deposits modified by erosive processes. The formation of thin beds of massive conglomerate in close proximity to aeolian deposits is likely related to deflation processes. Deflation surfaces were also described in the study area at the transition from fluvial to aeolian units (Zavala *et al.,* 2005; Veiga & Spalletti, 2007).

Quebrada del Sapo Formation: Aeolian facies association

Trough to planar cross-stratified sandstone facies

Description. This facies consists of trough or planar cross-stratified, well-sorted, fine to coarse-grained sandstone (Fig. 4C). Inversely graded intervals occur within the foresets, having a thickness of 0.5 to 5.0 cm. Foresets can dip as steeply as 32°. The cross-stratified sandstone occurs in medium (10 to 30 cm) to very thick (1 to 2 m) beds, showing internal reactivation surfaces. Palaeocurrent indicators are directed mostly towards the north-east and subordinately towards the north and east (N = 10). Locally, parallel-crested, low-amplitude ripples having a high ripple index (length/height of 20 to 25) are present. Towards the top, near the contact with the Vaca Muerta Formation, a 1 to 2 m thick sandstone interval shows convolute bedding and water-escape structures. Abundant, 1 mm wide pyrite cubes replaced by iron oxides and 5 to 10 cm wide carbonate concretions are present. This facies shows a thickness of 3 to 28 m.

Interpretation. Steep foresets, very good sorting and low-amplitude ripples characterize an aeolian setting. Although palaeocurrent data is limited, its low dispersion suggests that the sandstone succession possibly resulted from migration of barchanoid or transverse aeolian dunes (see also Zavala *et al.,* 2005; Veiga & Spalletti, 2007). Previous studies in the area have recognized third-order (reactivation), second-order (superimposition) and first-order (interdune) surfaces, indicating the development of composite draas formed by dunes (Zavala *et al.,* 2005; Veiga & Spalletti, 2007). Liquefaction towards the top of the succession resulted from the collapse of water-saturated sands experiencing mechanical loading during a water-table rise associated with marine flooding (e.g. Collinson, 1994).

Vaca Muerta Formation: Marginal-marine and shallow-marine facies association

Facies 1 (F1): Low-angle cross-bedded to horizontal-bedded sandstone

Description. This facies can be subdivided into two lithofacies. Lithofacies 1a (F1a) consists of sharp to erosive-based, thin to medium-bedded (3 to 20 cm thick), low-angle cross-bedded to horizontal-bedded, medium-grained with minor fine-grained sandstone (Figs 5A and 6). Asymmetrical and symmetrical ripples displaying a low index (length/height of 10 to 15) are common on bedding planes (Fig. 5B). The low-angle cross-bedding shows variable dips, but predominant slopes are towards the ESE and WSW, and subordinately towards the north and north-east (N = 6), whereas current-ripple foresets dip towards the south and WNW (N = 4, palaeocurrent data in Fig. 7B). Lithofacies 1b (F1b) comprises 10 to 30 cm thick, erosive to sharp-based, trough cross-stratified, medium-grained to minor coarse-grained sandstone (Fig. 5D). This lithofacies is locally observed at the base of or interbedded within F1a. In places, the sandstone exhibits organic matter drapes. Both lithofacies locally display water-escape struc-

tures and syn-sedimentary faults. The water-escape structures constitute 1 to 3 m of deformed strata that occur isolated or laterally associated with the low-angle cross-bedded sandstone (Fig. 5C). The synsedimentary normal faults exhibit displacements of centimetres to a few metres and associated drag folds, and they commonly cross-cut this facies and the underlying aeolian deposits of the Quebrada del Sapo Formation (Fig. 5D). F1a shows a tabular to subtle lenticular geometry that laterally grades into F1b (Fig. 6). At a large-scale, F1 displays a tabular geometry and thickness variations of 0.5 to 2.0 m.

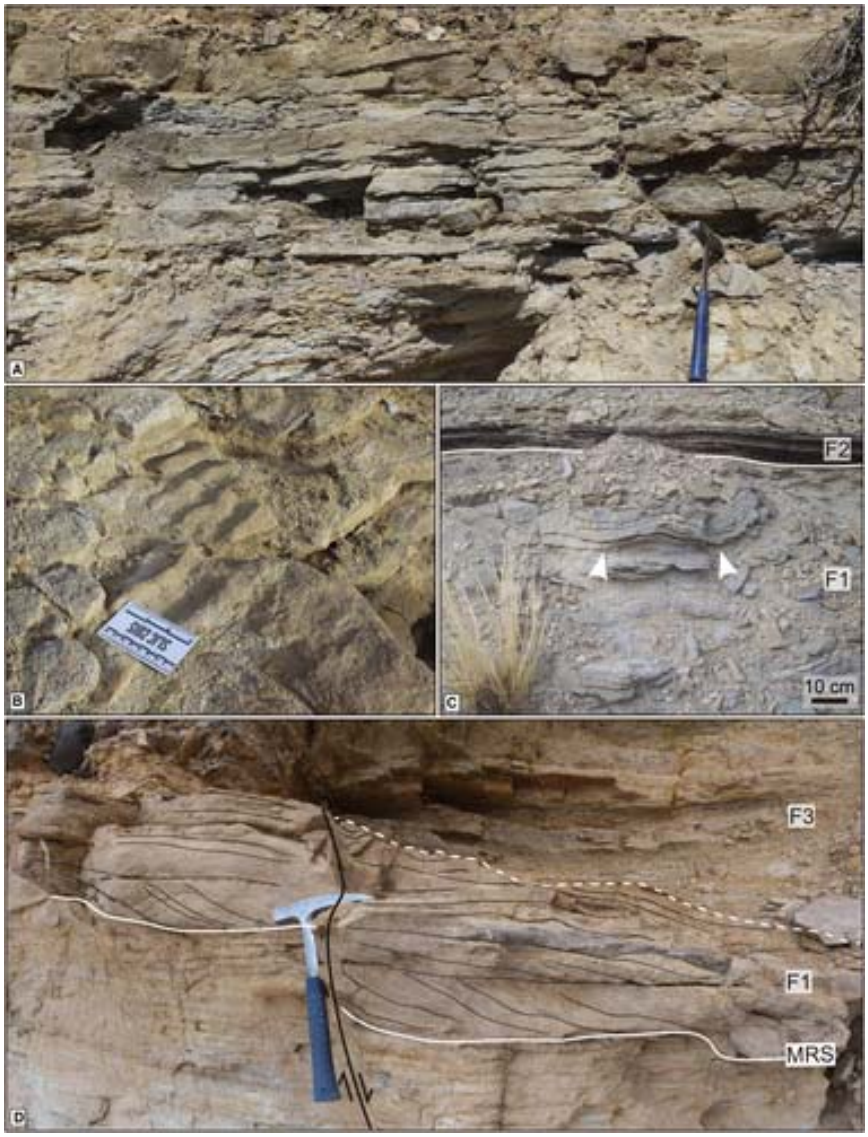

Fig. 5 Facies F1 of the Vaca Muerta Formation. (A) and (B) Low-angle cross-bedded sandstone overprinted by current ripples on bedding planes. (C) Water-escape structures in F1 (arrow), overlain by bindstone of F2. (D) Trough cross-bedded sandstone of F1 erosively overlying the aeolian facies association of the Quebrada del Sapo Formation. The contact represents a maximum regressive surface (MRS) cross-cut by a syn-sedimentary normal fault and overlain by facies F3 (hammer for scale is *ca* 30 cm long).

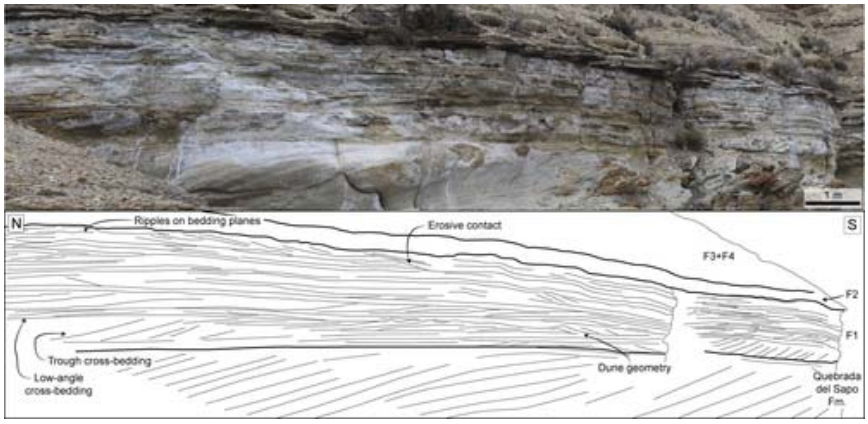

Fig. 6 Bedding planes and charac-teristics of F1. This facies sharply rests on the aeolian sand-stone suc-cession of the Quebrada del Sapo Form-ation, and it is covered by F2, F3 and F4.

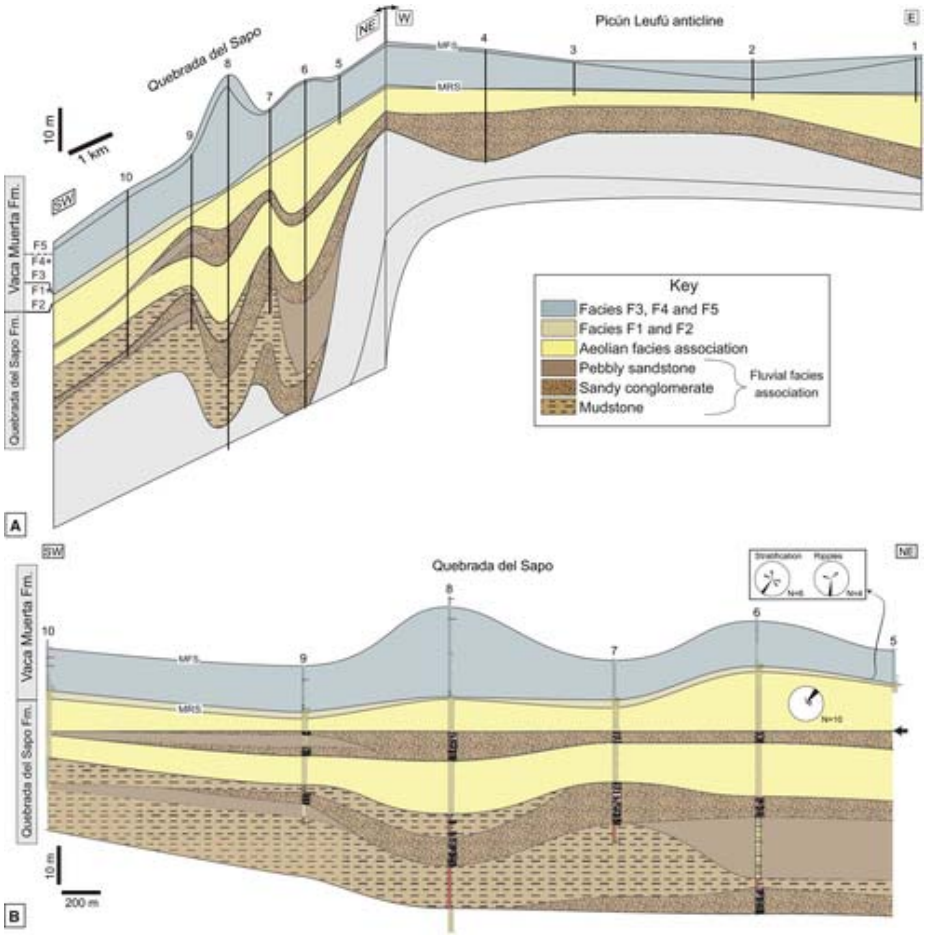

Fig. 7 Stratigraphic correlation of sections in the Picún Leufú domain (PL) and Quebrada del Sapo (QdS). (A) General correlation of the study area. (B) Stratigraphic correlation in the QdS, with the base of the last aeolian succession of the Quebrada del Sapo Formation drawn as horizontal reference level (arrow). Note thick-ness changes in the aeolian interval and the overlying TST succession.

Interpretation. Facies 1 documents episodic marine flooding and reworking of the Quebrada del Sapo Formation aeolian dune deposits in a beach area (for example, 'Laminated and Cross-bedded Sandstone facies' of Blakey *et al.,* 1983; or 'Planar-Bedded Sandstone lithofacies' of Desmond *et al.,* 1984). The subaqueous reworking is similar to wet interdune facies (Ahlbrandt & Fryberger, 1981; Kocurek, 1981), yet adjacent dunes are not preserved. F1a suggests low-relief bedforms that were later reworked into ripple surfaces by repeated flooding (e.g. Fryberger *et al.,* 1990). The lithofacies does not show bimodal sorting or inverse grading, precluding the hypothesis of aeolian climbing translatent strata. The low-index current ripples are typically produced in rather shallow centimetre-deep water (Tanner, 1967), whereas the symmetrical ripples indicate wave reworking. The water-escape structures suggest soft-sediment deformation of water-saturated sands. Lagoons adjacent to dune fields can expand over interdune areas during high water level and generate shallow-water, wind-induced wave reworking (Inman *et al.,* 1966; Shinn, 1973). These parts of the aeolian dune field show an enhanced preservation potential due to their position below the water table (Hummel & Kocurek, 1984). F1b may record the formation of small subaqueous dunes generated during marine flooding and scouring of beach deposits (Kocurek, 1981). Subaqueous tractive processes reworking the previous aeolian deposits generated segregation of the coarser grains into these bedforms. The organic matter drapes probably represent material reworked from the adjacent coastal areas (for example, F2). In modern settings, thin, cross-bedded and ripple cross-laminated sandstone beds having an erosional base and showing water-escape structures are typical of subaqueous marine reworking (Fryberger *et al.,* 1988). The erosive, irregular stratal contacts imply sand stabilization by damp conditions and later erosion during marine flooding. Synsedimentary normal faults cross-cutting F1 and the underlying Quebrada del Sapo Formation dune deposits suggest tectonic extension at the time of deposition.

Facies 2 (F2): Bindstone

Description. This facies comprises 5 to 30 cm thick bindstone beds (Figs 5D and 8A). Macroscopically, the bindstone displays dark, millimetre-thick, parallel to irregular, planar to wrinkle lamination. In thin section, the bindstone shows alternating wavy to lenticular, sand-rich and organic-rich laminae (Fig. 8B). The organic-rich laminae contain sand grains displaying a preferential orientation of their long axes parallel to lamination (Fig. 8B). Pyrite crystals occur abundantly aligned sub-parallel to stratification. The organic carbon content of the bindstone can reach 20% C_{org} (N = 2). Indistinct ammonite moulds and bivalve shells occur scattered in the bindstone.

Fig. 8 Bindstone of F2 (dark interval). (A) Outcrop, F2 overlying F1 (sandy interval at the base). Hammer for scale is *ca* 30 cm long. (B) Thin section of the bindstone showing alternating sand-rich and organic matter-rich laminae and oriented sand grains. Scale is 1 mm.

Interpretation. Facies 2 resulted from vertical accretion of microbial mats in a bay-margin area associated with an open-bay depositional environment (see below). The wavy to lenticular laminae are very similar to the wavy-crinkly laminated structure typical of microbial mats (Schieber, 1986, 2007). In addition, oriented grains and layered pyrite indicate microbial activity (Noffke, 2010). Similar microbial mats thrive in protected, transitional areas at the coast of the Guerrero Negro area, Mexico, yet they are related to hypersaline environments (Fryberger *et al.,* 1990).

Facies 3 (F3): Mudstone with interbedded sandstone layers, bioclastic wackestone and packstone

Description. This facies consists of cycles of thin-bedded (1 to 10 cm), carbonaceous–calcareous medium mudstone, bioclastic wackestone and packstone (Fig. 9A and B). Thin, gradational-based, medium to coarse-grained, calcareous sandstone occurs in PL (Fig. 9C), while 1 to 5 cm thick, muddy heterolithic beds are present in section 1. Symmetrical ripples occur locally in the bioclastic wackestone and medium to coarse-grained sandstone (Fig. 9B). The TOC content shows values of 2% and 17% (N = 2). In the medium mudstone, carbonate locally occurs as fine-grained mineral clusters in between millimetre-thick laminae of kerogen seams, whereas in the calcareous sandstone it is observed as matrix and cement. In the wackestone and packstone, debris and shells of bivalves, ammonites and gastropods are present. Well-preserved to fragmented bivalve (2 to 4 cm wide) and ammonite (5 to 20 cm wide) shells occur loosely packed (5 to 25%; Fig. 9D). Locally, ammonite shells have bivalves attached. These ammonite-rich and bivalve-rich beds are observed in all sections. In contrast, a

monospecific gastropod fauna was only encountered in the QdS (sections 5 to 10). It comprises well-preserved, 2 to 5 mm long and 1 to 2 mm wide shells (Fig. 9E), and highly fragmented shell debris, 0.1 to 0.5 mm in size. The gastropods occur in 1 to 5 cm thick beds either randomly or concordant to stratification, sparsely dispersed (2 to 5%) or loosely packed (10 to 15%). Bioturbation is recorded by poorly defined biodeformational structures, *Teichichnus rectus* (Fig. 9A) and *Thalassinoides* isp. A. Deposits containing biodeformational structures are moderately to intensely bioturbated (BI = 4 to 5), whereas those with discrete burrows tend to be slightly less bioturbated (BI = 3 to 4). A second generation of low density (BI = 1) *Thalassinoides*, referred to as *Thalassinoides* isp. B, cross-cuts all other trace fossils, has sharp, unlined walls and is passively filled by medium to coarse-grained sand (Fig. 9E and F). Laterally, F3 varies from 1 m to *ca* 2 m in thickness.

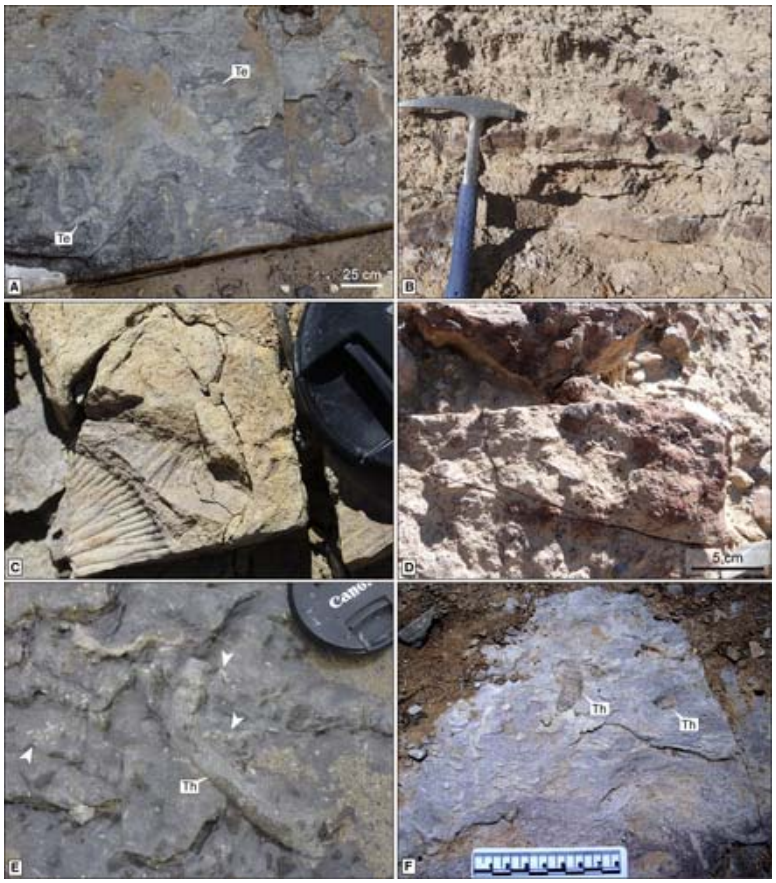

Fig. 9 Proximal bay facies. (A) Bioclastic wackestone exhib-iting monospecific oc-currence of *Teichichnus rectus* (Te). (B) Bioclastic wacke-stone to packstone showing symmet-rical ripples (hammer for scale is *ca* 30 cm long). (C) Medium to coarse-grained calcareous sand-stone (lens cap is 5.5 cm diameter), alter-nating with bioclastic wacke-stone showing ammonite moulds. (D) Close-up picture of the bioclastic wackestone showing fragmented to parti-ally preserved bivalves, am-monites and gastropods. (E) and (F) Bioclastic wackestone showing gas-tropods (white arrows), cross-cut by *Thalas-sinoides* isp. (Th) passively infilled by medium to coarse-grained sandstone.

Interpretation. Facies 3 formed at the margin of an open bay. The symmetrical ripples suggest oscillatory flow reworking associated with fair-weather or storm-wave action. The shell accumulations may indicate low sedimentation rates because low-energy winnowing of fines occurred during the transgression (Kidwell & Aigner, 1985). The sand grains of the calcareous sandstone were probably delivered by wind from the adjacent aeolian dunes or beach deposits (F1). The muddy heterolithic deposits are interpreted to have accumulated in a protected low-energy environment, where suspended particles settled down to the seafloor during tranquil periods. The millimetre-thick kerogen laminae and the high TOC content are typical of microbial mats that stabilized the substrate (Carmona *et al.*, 2011, 2012). Gastropods are similar to the cerithioid gastropods analyzed by Gründel & Parent (2001, 2006). The good preservation of some cerithoid gastropods and the absence of erosive surfaces below the shell beds imply their autochthony, whereas randomly disposed shells suggest minor reworking and parautochthony. The shell debris was probably delivered from higher-energy areas. Cerithioid gastropods have been reported from nearshore, mud-rich environments offshore southern

Vietnam (Szczucinúski *et al.,* 2013), from tidal flats in South Thailand (Waite & Strasser, 2011), and in the Bay of Bengal where they occur in high abundance and produce grazing trails (De, 2000). In addition, such gastropods are also associated with microbial mats thriving in the moist supratidal depressions (De, 2019). However, cerithioid gastropods, such as those belonging to the Turritellidae family, show a wide bathymetric range and can tolerate a broad range of salinity and temperature (Allmon, 1988). During microbial mat growth, the substrate below dewatered and became firm and, thus, suitable for exploitation by *Thalassinoides* producers that cross-cut the biodeformational structures. The sharp, unlined walls and the passive, allochthonous infill of *Thalassinoides* are diagnostic of the *Glossifungites* Ichnofacies, and indicate firmground conditions (Pemberton & Frey, 1985; MacEachern *et al.,* 1992). The coarse-grained sandstone infilling burrows probably originated from sand-rich flows that bypassed the area. These flows deposited their load in the distal-bay areas where sandstone beds are preserved (F4, see below). The absence of proximal, storm-generated shoreface or foreshore deposits, such as cross-bedded, parallel-laminated or hummocky cross-stratified sandstone, supports the above interpretation. Therefore, a low-energy, protected coast is suggested, and pronounced lateral thickness changes imply sedimentation rates varying along an irregular-shaped shoreline. An open-bay setting is more plausible than an estuarine environment because incised valley fill or flooded fluvial channel deposits are absent (MacEachern & Gingras, 2007).

Facies 4 (F4): Medium mudstone with interbedded greyish-green fine mudstone beds, sandstone beds and tuff layers

Description. This facies consists of grey, carbonaceous, medium mudstone showing subordinate 5 to 20 cm thick, sharp to erosive-based, greyish-green, fine mudstone beds, medium-grained sandstone and tuff beds (Fig. 10A, B and C). The TOC content is moderate (*ca* 2.5%; N = 2). The background carbonaceous mudstone displays abundant, 0.2 to 1.0 mm long, ellipsoidal to round-shaped pellets in the matrix, whereas the greyish-green mudstone contains pellets at the base. The sandstone is composed by organic-rich intraclasts of coarse-sand size located 1 to 2 cm above the base, giving an inverse to normal-graded appearance (Fig. 10B). Ammonite and bivalve shells are minor components of the mudstone. This facies is highly bioturbated, displaying biodeformational structures and discrete trace fossils, such as *Thalassinoides* isp.*, Palaeophycus tubularis, Teichichnus rectus* and *cf. Teichichnus patens* (Fig. 10D, E and F). The discrete trace fossils are seen in the basal part of a bed, where a distinct colour contrast between mudstone, sandstone and tuff intervals occurs (Fig. 10B). Locally, *Teichichnus rectus* constitutes monospecific occurrences (Fig. 10C and F). The burrows are 3 to 10 mm wide. The burrow boundaries of *Teichichnus* are sharp to irregular, and commonly show ellipsoidal pellets (Fig. 10F). The bioturbation index is 2 to 3 for intervals containing only discrete trace fossils and 5 to 6 if biodeformational structures occur. This facies is 2 to 10 m thick.

Interpretation. This facies is ascribed to a distal-bay environment where mudstone is indicative of low-energy, hemipelagic sedimentation. The greyish-green mudstone and medium-grained sandstone beds are interpreted as muddy tempestites and concentrated sand-rich density flows originating at the coast. The concentrated density flows eroded the underlying organic-rich mudstone and transported the mudstone mainly as intraclasts. Massive sandstone beds deposited by sandy mass flows occur in marine environments above aeolian successions, where storms erode adjacent aeolian systems and transport material seaward by subaqueous flows (Eschner & Kocurek, 1986). The muddy distal-bay deposits are similar to the sediments described from the central Eckernförde Bay in the south-west Baltic Sea, where laminated muddy tempestites and pelletized strata are interbedded (Bentley & Nittrouer, 1999).

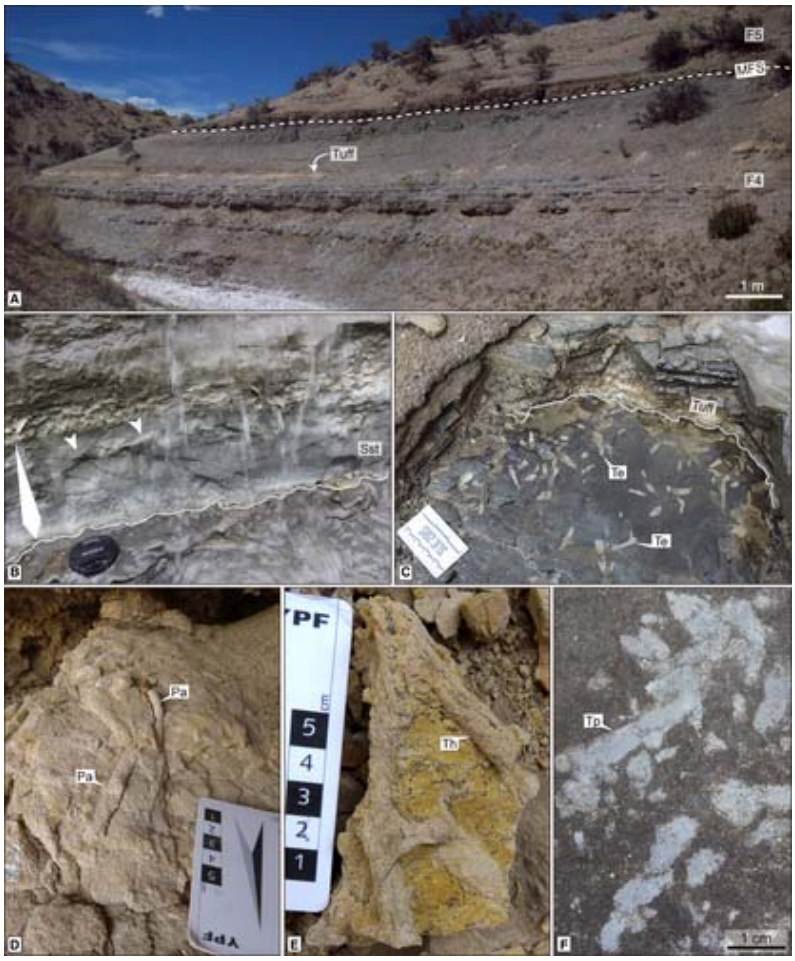

Fig. 10 Distal-bay facies (F4). (A) Outcrop showing the transition of F4 to the siliciclastic basin facies F5 while the supposed probable maximum flooding surface (MFS) is located in between. (B) Medium-grained sandstone (Sst) showing inverse to normal grading, with trace fossils originating from the overlying intervals (white arrows). Lens cap is 5.5 cm in diameter. (C) Tuff intervals passively infilling *Teichichnus rectus* (Te). (D), (E) and (F) *Palaeophycus tubularis* (Pa) and *Thalassinoides* isp. (Th) in intensely bioturbated intervals, and monospecific occurrences of *cf. Teichichnus patens* (Tp) with pellets along the wall.

The sharp burrow margins of *Teichichnus rectus* characterize a stiff to firm substrate. Furthermore, a stiffground scenario is indicated by the insignificant compaction of burrows in the fine-grained sediment (Wetzel & Uchman, 1998; Lobza & Schieber, 1999). The low ichnodiversity and moderate to high degree of bioturbation reflect an opportunistic population strategy that is characteristic of brackish-water environments (Pemberton & Wightman, 1992). Particularly, the monospecific, high-density occurrence of *Teichichnus rectus* is typical of marginal marine environments experiencing salinity fluctuations (Buatois *et al.,* 2005; MacEachern *et al.,* 2007; Díez-Canseco *et al.,* 2015). A similar lagoonal bay, nearshore setting was inferred from the abundant *Teichichnus* occurring in Middle Jurassic deposits of the North Sea (Petersen *et al.,* 1998), and in Lower and Middle Jurassic deposits of Denmark (Bromley & Uchman, 2003). In addition, the common occurrence of *Teichichnus* in bay and lagoonal facies associated with brackish waters has been extensively documented (Pemberton *et al.,* 2001; Buatois *et al.,* 2005). The absence of bay-mouth facies and the lack of other salinity fluctuation indicators such as, for example, trace fossil size reduction and syneresis cracks, suggest to assign these embayment deposits to an open rather than to a restricted bay (MacEachern & Gingras, 2007).

Facies 5 (F5): Parallel-laminated medium to fine mudstone

Description: This facies is the thickest facies of the Vaca Muerta Formation, yet the basal transgressive succession only is considered. It is composed of very thin-bedded, parallel-laminated medium to fine mudstone (Fig. 11A). Discontinuous, anastomosing, wrinkle laminae of kerogen seams are denser in the fine than in the medium mudstone. In the studied interval, the TOC content ranges between 1% and 12% (mean *ca* 5%; N = 5). Locally, sharp-based, 2 to

3 cm thick massive tuff layers occur (Fig. 11B). In both medium and fine mudstone, soft-sediment deformation structures include slumps, sand dykes and syn-sedimentary faults. Ellipsoidal, 20 to 70 cm long carbonate concretions occur, and become more abundant upsection. Moderate to high concentrations of well-preserved, flattened, 2 to 20 mm wide pectinid bivalve shells (*Huncalotis,* Damborenea & Leanza, 2016) are present on bedding planes. Some of the larger bivalves are spatially associated with ammonite shells. Ammonites, plant debris and fish scales are minor constituents. Ammonites are well-preserved to partially fragmented. Some specimens are up to 20 cm in diameter.

Fig. 11 Siliciclastic basin facies (F5). (A) Discontinuous, anastomosing, parallel lamination in the medium to fine mudstone produced by kerogen seams. (B) Unbioturbated tuff intervals (white arrows), which contrast with the tuff intervals occurring in F4 bioturbated by producers of *Teichichnus rectus* (scale in inches).

Interpretation: This facies formed in a basinal environment. High amounts of organic matter and kerogen seams, as well as the absence of macrofauna burrows, point to an at least temporary oxygen deficiency. The relative absence of event beds (sharp or erosive, discrete beds) indicates that the predominant processes were hemipelagic. In this sense, organic matter was provided by marine snow, whereas the silt grains of the medium mudstone were airborne (e.g. Gabbott *et al.*, 2010). Sand dykes and syn-sedimentary faults are related to gravity-driven mass movements that likely were triggered by the tectonic activity in the study area. The colour contrast provided by tuffs documents the absence of macrofaunal burrows (Fig. 11B; compare with F4, Fig. 10C). The lack of bioturbation structures implies oxygen deficiency of bottom and pore water. *Huncalotis* is found in upper Tithonian deposits of the Vaca Muerta Formation in the western–central Neuquén Basin, and is considered a pseudoplanktonic epibyssate living on swimming ammonites (Damborenea & Leanza, 2016). Bivalve shell pavements may reflect short-term benthic settlement representing an opportunistic strategy due to fluctuating oxygenation (Damborenea & Leanza, 2016), similar to some black shales in the Posidonia Shale of Germany (Röhl *et al.*, 2001). Because concretions need time to grow (e.g. Raiswell & Fisher, 2004), their strata-bound arrangement suggests intermittent sediment accumulation (Wetzel & Allia, 2000).

FACIES DISTRIBUTION AND SEQUENCE STRATIGRAPHY

Facies distribution can be differentiated into two areas: PL (sections 2, 3 and 4), and QdS and section 1 (sections 1, 5, 6, 7, 8, 9 and 10). In PL, the Quebrada del Sapo Formation continental deposits show a reduced development of fluvial and aeolian units (Fig. 7). Locally, a conglomeratic fluvial deposit with a deflation surface above occurs towards the top. The contact between the Quebrada del Sapo and Vaca Muerta formations is represented by a flat surface, overlying aeolian dune deposits (Fig. 12A) or locally the conglomeratic fluvial deposits. The

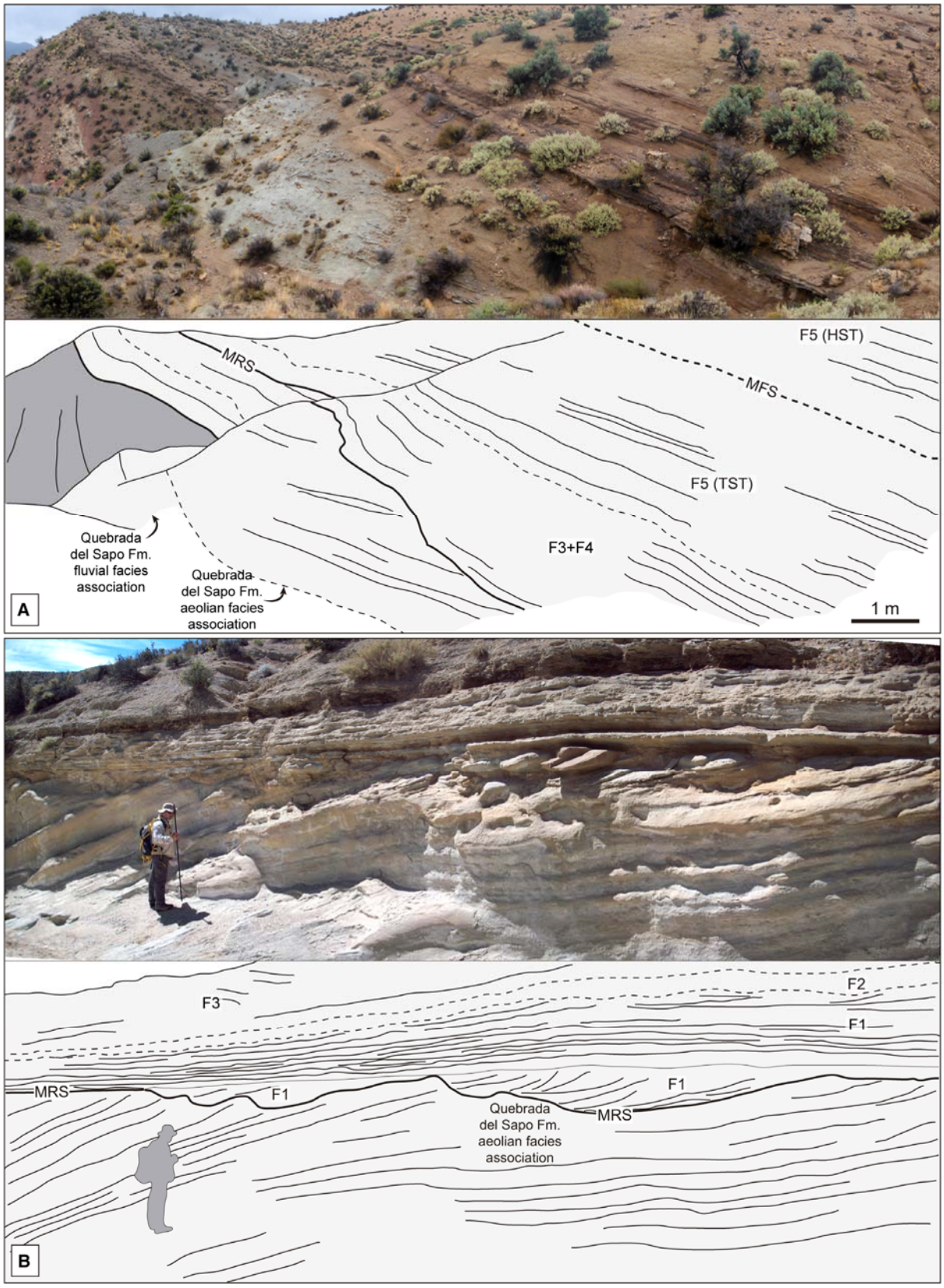

Fig. 12 Contrasting development of the Quebrada del Sapo Formation and the TST of the Vaca Muerta Formation in (A) topographic high areas located close to the Picún Leufú anticline (picture from section 4), and (B) low areas (Quebrada del Sapo, picture from section 10). Person for scale is ca 1.7 m tall.

entire sequence of the Vaca Muerta Formation shifts from bay-margin bindstone (F2) to shallow-marine (F3 and F4) sediments, comprising a retrogradational stacking pattern (F1 is not observed). Therefore, the contact between the Quebrada del Sapo and Vaca Muerta formations represents a maximum regressive surface (MRS) overlain by a Transgressive Systems Tract (TST). In places, the bindstone (F2) is not observed and proximal bay deposits (F3) rest on top of the contact. This TST is within the Virgatosphinctes mendozanus ammonite zone (Parent et al., 2011), which has been assigned to the late early Tithonian–early middle Tithonian (Riccardi, 2008). However, there is still considerable debate about the age of the Andean ammonite biozones (Vennari et al., 2014; Riccardi, 2015; Kietzmann et al., 2018).

In QdS, the Quebrada del Sapo Formation continental facies comprises two fluvial to lacustrine and two aeolian successions (Fig. 7; see also Zavala et al., 2005). Here, the contact between the Quebrada del Sapo and Vaca Muerta formations is variable depending on the scale of observation. In outcrops, the contact represents a planation to erosional surface and the previous dune relief is not preserved (Figs 6 and 12B). However, at a larger scale, the topography of partially preserved megadunes constitutes a reworked relief. This topography is evidenced by minor thickness changes in the Quebrada del Sapo Formation, that can be observed when the strata correlation is normalized to the deflation surface at the base of the last aeolian interval (Fig. 7B) (top of unit T3 of Zavala et al., 2005). The aeolian interval is thicker in sections 6, 8 and 10 (15.2 m, 8.3 m and 8.4 m, respectively) and thinner in sections 7 and 9 (6.3 m). F1 and F2 are thicker in sections 7, 9 and 10 (1.7 m, 1.8 m and 1.9 m) and thinner in sections 6 and 8 (0.4 m and 1.1 m). Thus, the thickness of the aeolian deposits is slightly inverse to the thickness of F1 and F2. F3 and F4 vary between 8.2 m and 22.8 m in thickness, and exhibit no relation to the thickness of the aeolian deposits.

Beach (F1), bay-margin (F2), proximal bay (F3) and distal bay (F4) deposits of the Vaca Muerta Formation occur on top of the planation to reworked contact in QdS and section 1. Similarly, as in PL, the retrogradational pattern suggests a TST overlying a MRS occurring at the base of F1. Basin facies (F5) mantles all of the underlying facies in both PL and QdS. In the first 1 to 3 m of F5, a level with carbonate concretions occurs, indicating condensation due to the development of a maximum flooding surface (MFS) and marking the top of the TST.

DEPOSITIONAL MODEL

The sedimentological and ichnological observations form the base to develop a depositional model for the aeolian to marine transition of the Quebrada del Sapo and Vaca Muerta formations in the study area (Figs 13 and 14). A decrease in thickness towards PL in both the Quebrada del Sapo Formation (23 to 62 m in QdS to 10 m in PL) and Vaca Muerta Formation (9 to 25 m in QdS to 5 to 9 m in PL; Fig. 7; Zavala & Freije, 2002) suggests the existence of topographically higher domains with lower accommodation rate in this area. One hypothesis considers that this topographic difference originated from the extensive tectonic activity of the anticline. Palaeocurrent indicators in fluvio-lacustrine deposits and detrital zircon ages suggest that the anticline constituted a source area prior to the deposition of the aeolian unit (Zavala & Freije, 2002; Zavala et al., 2005, 2008; Naipauer et al., 2012). The progressively developed unconformities of the Picún Leufú anticline indicate continuous deformation throughout deposition of the Quebrada del Sapo and Vaca Muerta formations (Fig. 12A; Freije et al., 2002; Naipauer et al., 2012). Particularly, deformation is expressed as a change of dip (2 to 17°) between the Quebrada del Sapo and Vaca Muerta formations, and as normal faults affecting the uppermost Quebrada del Sapo Formation (Fig. 5D; Freije et al., 2002, fig. 11A), indicating tectonic influence during the transgression. A second hypothesis implies that the topographic difference is related to a different position within an erg, with the higher domains (PL) occurring

in the centre of the erg (Veiga & Spalletti, 2007). The relative constant thickness of the uppermost fluvial and aeolian units of the Quebrada del Sapo Formation supports this idea, with less influence of tectonics towards the end of continental deposition (Fig. 7A).

The pre-transgression topography of the aeolian dune field affected facies distribution and sediment accumulation of the Quebrada del Sapo and Vaca Muerta formations (Fig. 7A). Both the fluvio-lacustrine and aeolian successions suggest alternating wet and dry conditions during deposition of the Quebrada del Sapo Formation in the study area. Many studies of this formation arrived at a similar environmental interpretation (Parker, 1965; Digregorio, 1972; Leanza & Hugo, 1997; Freije et al., 2002; Zavala & Freije, 2002; Zavala et al., 2005, 2008; Spalletti & Veiga, 2007; Veiga & Spalletti, 2007). Increasing accommodation space towards the low domains of QdS, enhanced by tectonic loading effects, generated thicker continental successions and development of lacustrine deposits. Predominance of aeolian facies towards the top implies increasingly arid and dry conditions that might have resulted from the growth of the Andean magmatic arc or lowering of water table due to basin compartmentalization (Veiga & Spalletti, 2007). Veiga & Spalletti (2007) suggested a shallower water table because the thickness of the aeolian dune field decreased towards the Chacaico–Charahuilla area (7 km south of QdS), located in an upwind erg-margin position.

The pre-transgression continental environment was characterized by transverse dunes oriented north-west/south-east that migrated towards the north-east (Fig. 14A; Zavala et al., 2005; Veiga & Spalletti, 2007). The existence of a topographic high in the Picún Leufú anticline suggests that the coast advanced from the south. Flooding of the sand source areas located to the south might have decreased the continental sand budget of the study area, leading to the partial destruction of the aeolian dune field (Eschner & Kocurek, 1988). However, the oblique orientation of the dunes with respect to the coast counteracted the destructive processes by restricting the area of dune erosion, therefore promoting preservation of the aeolian palaeotopographic relief (Eschner & Kocurek, 1988).

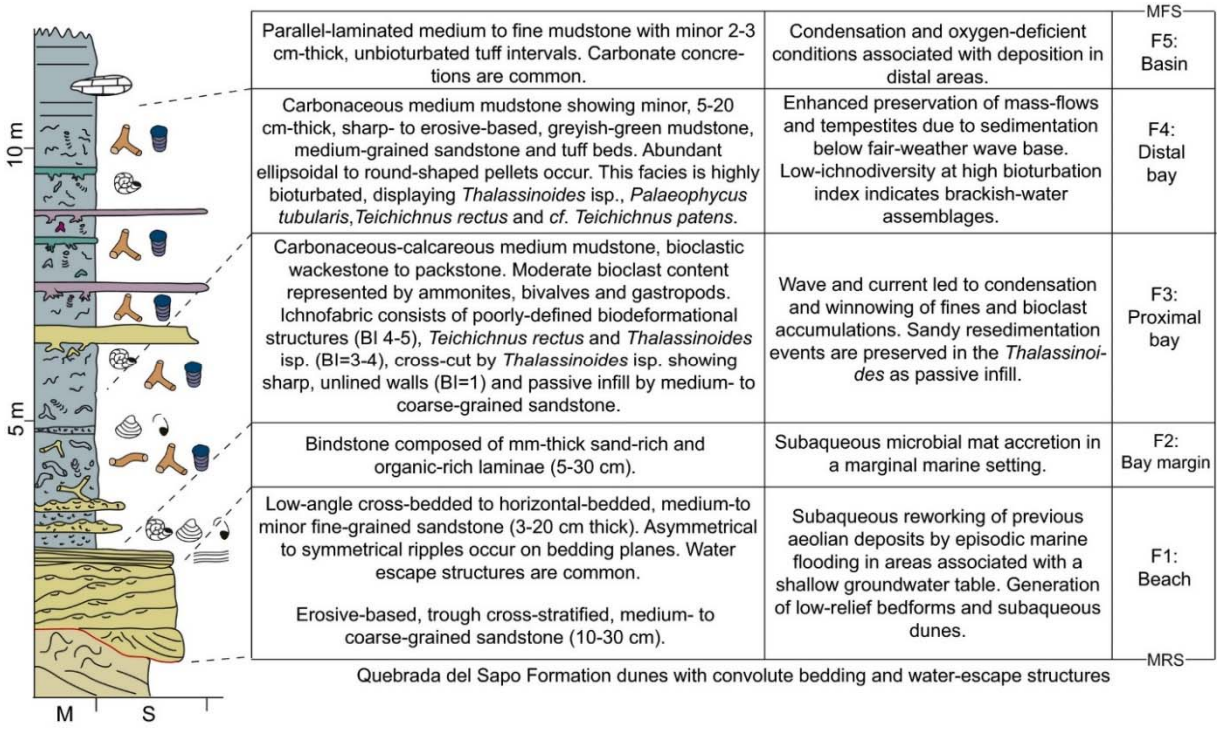

Fig. 13 Idealized depositional evolution of the Vaca Muerta Formation transgressive succession. Key in the stratigraphic sections of the Supporting Information.

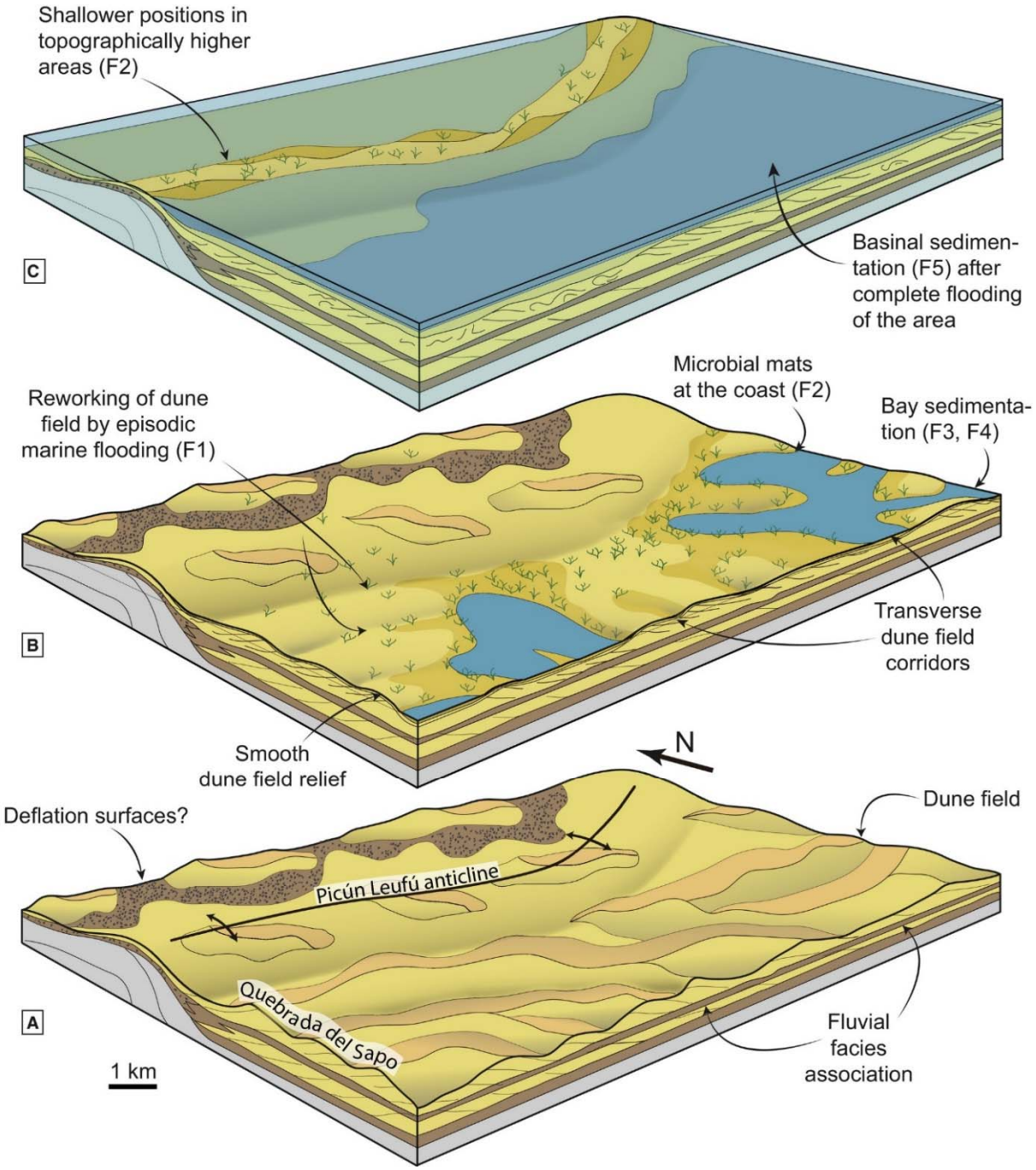

Fig. 14 Depositional model of the Vaca Muerta Formation transgression showing: (A) the pre-flooding topography; (B) the transgressive coast; and (C) the complete flooding of the study area.

The reworked to planated MRS indicates that the record of the last stage of aeolian accumulation in the Quebrada del Sapo Formation was partially eroded. The monotonous aeolian dune facies with soft-sediment deformation is the typical deposit below the MRS, yet locally, other facies were documented. In section 2, the top of the Quebrada del Sapo Formation shows deflation processes overlying the aeolian dune deposits. Sand sheet deposits occur above the last aeolian dune units in a location close to section 1 (Veiga & Spalletti, 2007). Deflation surfaces and sand sheets overlying the uppermost aeolian dune deposits and below the MRS were also recorded

30 km to the north-east of the study area (fig. 16 of Cevallos, 2005). All of this evidence suggests a switch towards a negative sediment budget at the end of the aeolian dune field phase, associated with the regional rise of the water table caused by the transgression. However, Veiga & Spalletti (2007) described an overall drying upward succession of the Quebrada del Sapo Formation for the study area, indicating that deflation observed at the top might be unrelated to the transgressive event, and represents a local process.

The transgression began with a base-level rise affecting the continental water table inland (Kocurek et al., 2001). The occurrence of soft-sediment deformation structures in the aeolian dunes located below the Vaca Muerta Formation indicates that water table rise caused by the marine flooding affected unconsolidated aeolian sand (F1). The continuous flooding by seawater and probably the negative sediment budget of the aeolian dune field associated with a flooded source area generated a large-scale reworked surface (sensu Eschner & Kocurek, 1988; Fig. 7B). The distance between the sections suggests a low-relief palaeotopography characterized by ridges with widths of ca 1500 m and heights of 2 to 9 m (Fig. 7D), interpreted to be megadunes (e.g. Cevallos, 2005). Minor scouring by channelized subaqueous dunes (F1b) caused by episodic flooding locally generated an erosive surface at an outcrop scale. In the elevated domains (PL), similar processes might have formed a planation surface (sensu Eschner & Kocurek, 1988).

As the coast retreated, beach processes reworked the preexisting Quebrada del Sapo aeolian dunes (F1; Figs 7B and 12B). The marine flooding also fostered soft-sediment deformation structures within this facies. During F1 deposition, the Quebrada del Sapo Formation dunes were stable as syn-sedimentary normal faults cross-cut the dunes. Low-relief beach bedforms developed while aeolian dune construction was hindered by wave erosion and damp sediment being stabilized by capillary forces. Recurrent marine flooding may have characterized this transition, generating demanding conditions for the benthos and, thus, preventing burrowing by macro-organisms. Microbial mats (F2) established in the transitional zone between the beach and the coastline (Fig. 14B). The microbial mats also facilitated preservation of aeolian and beach deposits by binding and covering them.

On top of F1 and F2, proximal bay deposits (F3) accumulated above fair-weather wave base. The proximal bay was a low-energy, sheltered embayment protected against strong waves and storms and does not show proximal shoreface facies, such as cross-bedded or HCS sandstone. Abundant fragmented or complete ammonite and bivalve shells became enriched due to winnowing of fines by waves. The producers of Thalassinoides, Palaeophycus and Teichichnus record a suspension-feeding/passive-predation or deposit-feeding mode that indicates the presence of nutritious particles in suspension and on the seafloor, respectively (Buatois & Mángano, 2011). Microbial mats probably stabilized the sediment and favoured the development of a stiffground later exploited by burrowing organisms. Sandy flows bypassed the area as recorded by the passive infill of the Thalassinoides. F3 marks the onset of marine processes above fair-weather wave base, and therefore its base constitutes a wave ravinement surface. The low-energy nature of the ravinement surface is supported by the absence of the Glossifungites Ichnofacies at F3 base, which is a distinguishing feature of high-energy wave ravinement erosive surfaces (MacEachern et al., 1992, 2012).

Continuous sea-level rise triggered deposition of the distal-bay facies (F4), composed of predominant hemipelagic sediments and intercalated event beds. In the distal bay, large amounts of mud accumulated in the turbidity maximum. The existence of sandy mass-flows in the distal bay suggests that unconsolidated aeolian dunes occurred adjacent to the coast (Eschner & Kocurek, 1986). Low ichnodiversity and a high degree of bioturbation indicate an opportunistic

population strategy typical of brackish-water environments. Further up, increasing distance to the coast led to decreasing sediment accumulation. Siliciclastic basinal deposits (F5) contain high amounts of organic matter and document oxygen-deficient conditions, evidenced by the absence of burrowing organisms. The interval ends with strata-bound carbonate concretions and associated indicators of lowered, intermittent sedimentation, marking the end of the transgression at the maximum flooding surface (MFS).

DISCUSSION

Current hypotheses about the transgression of the Vaca Muerta Formation

The current hypothesis for the Vaca Muerta Formation transgression envisages an instantaneous catastrophic Tithonian flooding preserving the aeolian fields (Mutti et al., 1994; Cevallos, 2005). This hypothesis relies on four main lines of evidence: (i) relative absence of onlap relationships to the underlying continental LST deposits (Cevallos, 2005); (ii) lack of transitional facies between the aeolian and marine deposits (Mutti et al., 1994); (iii) preservation of the underlying dune-field topography indicating subordinate marine reworking (Cevallos, 2005; Reijenstein et al., 2014; Acevedo & Bande, 2018); and (iv) presence of soft-sediment deformation structures in the upper part of the aeolian deposits (Cevallos, 2005; Veiga & Spalletti, 2007).

In the Neuquén Basin, catastrophic transgressions were interpreted at different basin-filling episodes. The catastrophic transgression of the Vaca Muerta Formation was described at the Dorsal de Huincul, 30 km north-east of the study area (Cevallos, 2005). There, the upper beds of the aeolian Kimmeridgian deposits (Catriel Formation) show liquefaction structures generated by flooding over unconsolidated deposits (Cevallos, 2005). The megadune topographic relief is preserved below the transgressive surface (Cevallos, 2005; see also Reijenstein et al., 2014; Acevedo & Bande, 2018). Overlying the transgressive surface, the TST consists of a few centimetres to >10 m thick succession of marl, black mudstone and limestone with bivalve bioclasts and siltstone and fine-grained sandstone intraclasts, named as the Rapid Transgression Remnant. This succession is covered by a 20 to 40 m interval of dark, laminated mudstone, referred as VM-A (Cevallos, 2005). The TST was interpreted to have been formed by sedimentation of the coarser-grained material because of subordinate reworking in its lower part, and by suspension fallout in its upper part (Cevallos, 2005). A catastrophic transgression was also suggested for the Lower Cretaceous Lower Troncoso Member of the Huitrín Formation based on the preservation of an aeolian palaeorelief and existence of subaqueous mass flows produced by reworking of unconsolidated sediment (Strömbäck et al., 2005; Argüello Scotti & Veiga, 2015).

The sections studied in this work provide clear evidence of a TST composed of retrograding beach, open-bay and siliciclastic-basin facies (Fig. 13), followed by prograding siliciclastic-basin facies. Facies transitions are indicated by: (i) beach deposits revealing a shallow groundwater table at the beginning of the flooding; (ii) microbial mats at the coast; (iii) symmetrical ripples recording wave reworking of proximal bay deposits; and (iv) aggradation of distal-bay deposits with alternating infaunal communities, as recorded by trace fossils. Therefore, the transgression occurred during a time span lasting long enough to allow the establishment of transitional environments and biotas. This time span is not consistent with a catastrophic transgressive scenario, where the coast migrates at a rate of kilometres per day (see below).

Another issue with the current hypothesis of the transgression is that preservation of an aeolian landscape is not restricted to catastrophic flooding, but it is also facilitated by a low-energy transgression in embayments (e.g. Jennings, 1975) or submergence of early-stabilized dunes (e.g. Al-Hinai et al., 1987; Carmona et al., 2012; Hanebuth et al., 2013; see review by Eschner & Kocurek, 1988). For instance, in the Fitzroy Delta in King Sound, Australia, low-energy, tidal-flat environments migrate over Quaternary aeolian dunes during the rapid Holocene marine transgression (Jennings, 1975). Stabilization by vegetation and a cover of tidal-flat mud favour the preservation of the dune topography (Jennings, 1975). In addition, early cementation of coastal dunes is promoted by groundwater seepage (Pye, 1983; Kocurek & Nielson, 1986; Chan & Kocurek, 1988). Microbial mats also stabilize the sediment and promote preservation of the transgressive deposits (Carmona et al., 2011, 2012).

Dune-field relief preservation has to be differentiated between megadune and dune relief, because the former constitutes a large-scale bedform commonly preserved in the rock record (for example, Fig. 7B), whereas the latter is hardly preserved in modern and ancient settings. A well-documented example of dune preservation is the Jurassic Entrada Formation, USA (Ahmed Benan & Kocurek, 2000). In the study area, dunes are not completely preserved because a sharp surface truncates their top at outcrop scale (Figs 6 and 12B), yet a megadune relief can be observed at a larger scale (Fig. 7B). Similar preservation of aeolian relief has been observed during different basin-fill stages of the Neuquén Basin (Cevallos, 2005; Strömback et al., 2005; Reijenstein et al., 2014; Argüello-Scotti & Veiga, 2015; Acevedo & Bande, 2018).

Another issue with the current hypothesis is that soft-sediment deformation structures not only result from a catastrophic transgression; they just indicate unconsolidated sediment, and they do not document the rate of coastline migration. A rise of the groundwater table facilitates soft-sediment deformation in the wet, highly porous, aeolian dune sand (see review by Doe & Dott, 1980; Kocurek et al., 2001).

To summarize, the findings of the present study do not support the previous hypothesis of an instantaneous catastrophic flooding for the Vaca Muerta Formation. The transgressive deposits clearly differ from ancient examples of catastrophically flooded dune fields as substantiated by three examples: (i) lower Permian Weissliegend Sandstone of Europe (Smith, 1979; Blaszczyk, 1981; Glennie & Buller, 1983; Strömbäck & Howell, 2002); (ii) Jurassic Entrada Formation, USA (Tanner, 1970; Vincelette & Chittum, 1981; Ahmed Benan & Kocurek, 2000; Kocurek et al., 2019); and (iii) Cretaceous Lower Troncoso Member of the Huitrín Formation, Argentina (Strömbäck et al., 2005; Argüello Scotti & Veiga, 2015). These examples contrast with the Vaca Muerta Formation in three aspects:

1 Reduced or absent coastal or marginal-marine facies transitions.

2 Mass-flow deposits originating from sediment shedding from dunes.

3 A relatively higher degree of aeolian relief preservation.

In contrast, the studied case shows an aeolian to marine transition consisting of coastal and marginal-marine environments (beach and bay deposits) similar to ancient examples of gradual transgressions (e.g. Blakey et al., 1983; Desmond et al., 1984). Considering the degree of aeolian palaeotopography preservation, the transition to the Vaca Muerta Formation is an intermediate case between gradual and catastrophic, with a planation to erosive relief observed at an outcrop scale (i.e. no dune-relief preservation, Fig. 12B), but megadune preservation at a large scale (Fig. 7).

Revised scenario for the transgression of the Vaca Muerta Formation

In the study area, during the transgression of the Vaca Muerta Formation a low-energy, embayed facies migrated rapidly over the continental deposits of the Quebrada del Sapo Formation. A rapid marine transgression is implied by the thin coastal deposits (F1, 0.5 to 2.0 m thick) prior to open-bay sedimentation and the absence of punctuated shoreline movements that would record a gradual transgression associated with a retrogradational parasequence set (Cattaneo & Steel, 2003). Erosion by wave reworking and deflation on the one hand, and stabilization provided by microbial mats and early cementation on the other hand, controlled the preservation of the aeolian relief. In seismic sections, the lack of onlap relationships and the absence of retrogradation represent additional evidence for a rapid transgression draping the basin topography (Cevallos, 2005).

The sharp basal MRS overlying the aeolian deposits of the Quebrada del Sapo Formation represents the first expression of the transgression. Deflation and marine flooding might have generated the planated to reworked relief. A good analogue to illustrate marine reworking of aeolian sediments is the western coast of Baja California near Guerrero Negro, Mexico (Fryberger et al., 1990). In this area, marine deposits truncate underlying aeolian cross-bedded deposits, commonly modified by water-escape structures or slumping during short-term flooding (Fryberger et al., 1990). Marine transgressive scouring of cemented aeolian strata formed an irregular erosional surface similar to that at the base of the trough cross-bedded sandstone (F1). In addition, subaqueous wave reworking comparable to F1 occurs within the interdune areas during episodic marine flooding (Inman et al., 1966).

The beach deposits are replaced by bay-margin facies characterized by microbial mats, similar to the Holocene transgression of the carbonate coast of Abu Dhabi, United Arab Emirates, where reworked aeolian deposits are covered by microbial mats (Strohmenger et al., 2010). The open-bay scenario for the Vaca Muerta Formation matches the observation of low-energy, non-incised, transgressive lithosomes that lack barrier facies and proximal shoreface facies. The reduced thickness of the open-bay sediments and the absence of progradational stacking patterns indicate a continuous transgression (Cattaneo & Steel, 2003). Within the embayment, the environmental conditions showed high lateral variability that is also typical of transgressive successions.

The low-energy, rapid transgression of the Vaca Muerta Formation could have evolved in an open bay similar to the Fitzroy delta of King Sound, Australia (Jennings, 1975; see above). Marginal-marine conditions established in corridors traversing the megadunes and fostered later inundation of the megadune crests (Fig. 14B; e.g. Jennings, 1975; Carmona et al., 2012). According to this scenario, it was possible to preserve the smoothed, reworked long-wavelength megadunes observed in the Dorsal de Huincul (Cevallos, 2005). The thin strata of the TST indicate a low-gradient transgressive surface (e.g. Ghinassi, 2007) that facilitated high rates of coastline migration. A modern example of a transgression over a gently sloped area is the Gulf of Tonkin, South China Sea; there, the coastline prograded over 700 km in 12 kyr while the transitional deposits are gradational and bioturbated (Wetzel et al., 2017), similar to those deposits documented in connection with the wave ravinement surface at F3.

Timing of marine transgressions over dunefield deposits

Considering the rate of landward migration of the coastline, aeolian to marine transitions can be subdivided into three main categories: catastrophic, rapid and gradual. The rate of coastline migration is controlled by the rate of sea-level rise and the slope of the transgressive surface.

This rate affects the preservation of the dune topography by the time available for marine reworking (Chan & Kocurek, 1988; Eschner & Kocurek, 1988), whereas the slope of the transgressive surface controls the accommodation space for transgressive deposits.

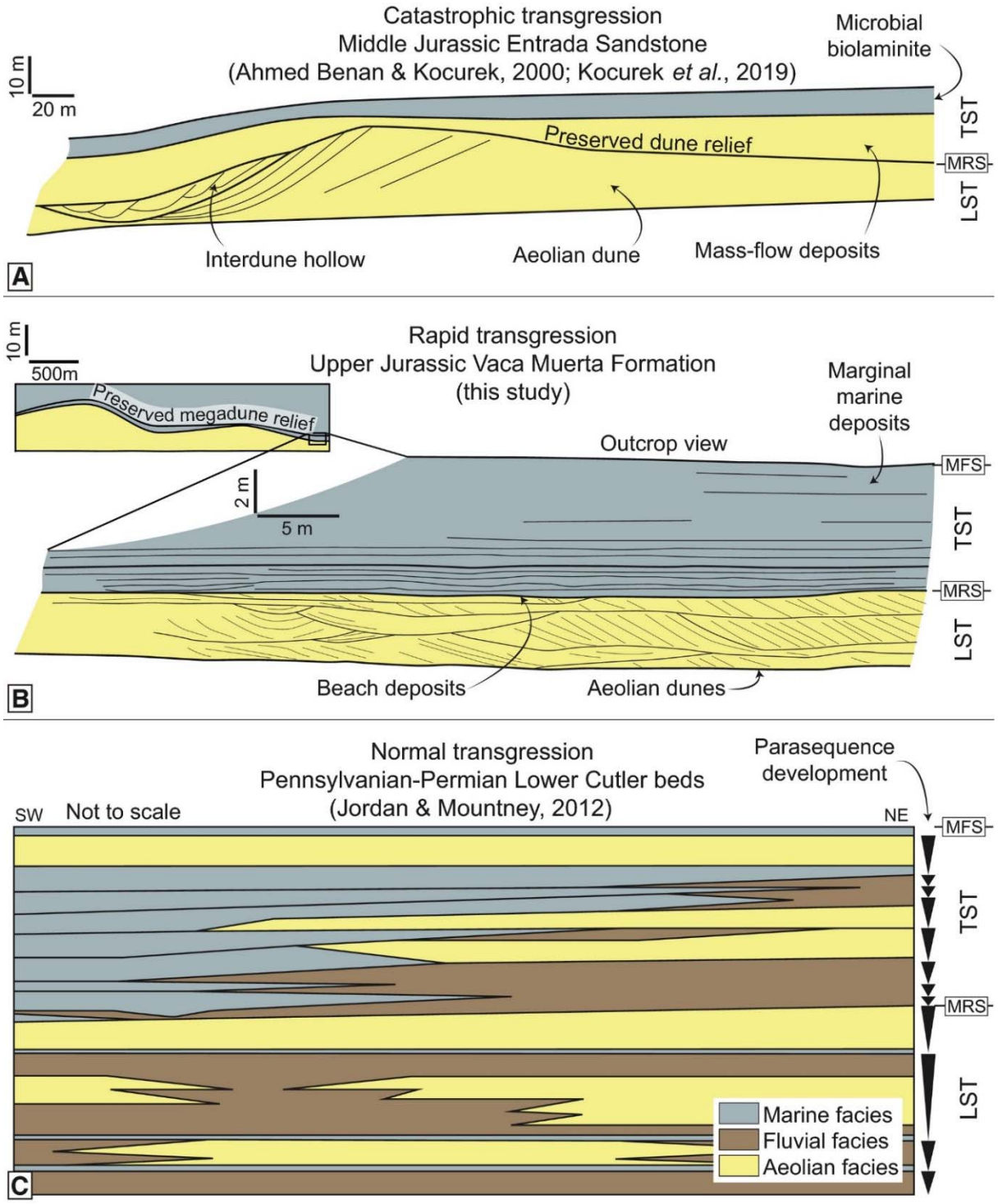

Fig. 15 Stratigraphic representation of three different transgressive scenarios over aeolian dune fields: (A) catastrophic; (B) rapid; and (C) gradual.

The sediment record of aeolian to marine transitions during catastrophic transgressions shows a limited representation of coastal or marginal-marine transitional settings (for example, shallow marine reworking associated with sudden flooding), high preservation of the aeolian landscape, and eventually sandy mass-flows shed from dunes (Fig. 15A). A catastrophic transgression occurs if the rise of water level is in the range of several metres during one to ten years caused, for instance, by sill or dam-breaks. This type of flooding requires that the water level within the basin is considerably below current eustatic sea level. A representative example is the catastrophic Zanclean flood filling the Mediterranean Sea at the end of the Messinian dry period (5.32 Ma; Blanc, 2002). Peak rates of sea-level rise could have exceeded 10 m day−1 (Garcia-Castellanos et al., 2009). High rates of sea-level rise are also suggested for the Holocene catastrophic flooding of the Black Sea (tens of centimetres per day; Ryan et al., 1997), although this is still a matter of discussion (Yanko-Hombach et al., 2007, and references therein). Assuming the rates of sea-level rise suggested by Garcia-Castellanos et al. (2009), a coastal plain sloping at 0.5 m km−1 (a value typical of low-gradient continental shelves; Harris & Macmillan-Lawler, 2016) would generate shoreline migration rates of kilometres per day.

Rapid transgressions in the range of the Holocene rates of sea-level rise lead to a thin TST composed of coastal or marginal-marine deposits that records the complete transition from aeolian to marine facies and may preserve the aeolian landscape relief (Fig. 15B; e.g. Jennings, 1975; Steele, 1983). Holocene rates of sea-level rise are of several to several tens of metres on timescales of 102 to 103 years, as for example after the Last Glacial Maximum when sea-level rise was on average 4.1 to 13.3 mm yr-1 and peak rates reached 1.25 to 5.33 cm yr−1 (Hanebuth et al., 2000, 2009; Yokoyama et al., 2001). On gentle slopes, these rates result in fast landward migration of the coastline. For example, the Holocene transgression (20 to 8 kyr) in the Gulf of Tonkin, South China Sea, caused an average coastline migration of 60 m yr−1 for a low-gradient shelf (ca 0.2 m km−1) and up to 150 m yr−1 for the Red River incised valley area (Wetzel et al., 2017). In this case, the rapid transgression resulted in low sediment supply to coastal and offshore areas. Therefore, commonly less than metre-thick deposits accumulated outside incised valleys, while inside the valleys tidal bars or coastal barriers did not form due to shortage of sand (Wetzel et al., 2017). Dune field topography (in the scale of megadunes) can be preserved if the coastal processes are of low-energy, as encountered at estuarine or embayed coasts (e.g. Jennings, 1975; Wetzel et al., 2017). Because a lower rate of landward migration leads to increased dune-field reworking, preservation of the dune field relief might be lower than in catastrophic transgressions.

Gradual transgressions over aeolian systems show low rates of coastline migration, and are only known from the sediment record. Most gradual transgressions lead to formation of retrogradational parasequence sets (punctuated transgressions of Cattaneo & Steel, 2003). They comprise several inland marine incursions and, thus, interbedded aeolian and marine deposits occur recurrently (e.g. Havholm & Kocurek, 1994; Blakey et al., 1996; Jordan & Mountney, 2010, 2012; Rodríguez-López et al., 2012). In addition, these transgressions record a rising groundwater table and upward increasing humid conditions on the continent, as evidenced by the switch to fluvial deposits (e.g. Jordan & Mountney, 2010, 2012). During that time, dunes below supersurfaces became stabilized and aeolian sedimentation resumed. An erosional relief may indicate a prolonged time span that allowed reworking of the aeolian topography by continental and marine processes (e.g. Moore, 1983; Huntoon & Chan, 1987). Therefore, gradual transgressions are recorded by transitions towards marine environments characterized by short seawater incursions (parasequences of 400 kyr; Jordan & Mountney, 2012) and preservation of planation surfaces or reworked relief towards the top of the aeolian succession. Marine and aeolian facies are interbedded (Fig. 15C).

The transition from the Quebrada del Sapo to the Vaca Muerta Formation resembles the sediment record of a Holocene rapid transgression at high rates of sea-level rise. Using sedimentation rates of modern estuarine systems as a measure (Nichols, 1989, and references therein), the basal TST of the Vaca Muerta Formation could have formed during a period lasting about 104 to 105 years. The calculation considers a compaction of 70% for the Vaca Muerta Formation estimated from the laminae bent around early diagenetic concretions, formed within the deposits of the 23 m embayment succession accumulated during TST (section 8). Thus, Holocene rates of sea-level rise can result in such a flooding scenario.

The proposed rates of sea-level rise in the range of the Holocene ones for the Late Jurassic face the problem of reconciling this data with the Jurassic sea-level curve (Haq, 2018). The global maximum sea-level highstand of the Jurassic occurs in the late Kimmeridgian–early Tithonian (Haq, 2018), slightly pre-dating the Vaca Muerta Formation. In the Neuquén Basin, therefore, compaction-induced, tectonic and/or thermal subsidence has to be taken into account to explain the discrepancy in the global sea-level chart with respect to the timing of the transgression. The Vaca Muerta Formation formed during the initial Aluk deformation stage, which represented the time of maximum areal extent of the deformation in the Dorsal de Huincul (Mosquera et al., 2011). The Vaca Muerta transgression was nearly simultaneous with an extensional phase of the Picún Leufú anticline (Freije et al., 2002), as documented by syn-sedimentary normal faults cross-cutting the contact between Quebrada del Sapo and Vaca Muerta formations. In addition, based on biostratigraphy and palaeobathymetric calculations, the Mesozoic rates of sea-level change were estimated to have had a magnitude of several metres to tens of metres per Myr (Immenhauser, 2005), supporting the idea that subsidence must have contributed to the high rates of relative sea-level rise in the study area. However, glacio-eustasy was also suggested to have occurred during the Mesozoic while modulated by high-altitude perennial ice shields (Immenhauser, 2005), which can result in similar rates of sea-level variations as in the Holocene. The origin of the transgression is still contentious and needs further investigations to understand which variable accounted for such rates of sea-level change.

The hypothesis of a rapid, Holocene-like transgression questions the current idea of a catastrophic transgression. A normal evolution of the Tithonian transgression in the Neuquén Basin has been proposed previously by Boll & Valencio (1996) and recently by Ponce et al. (2015, 2016). This is consistent with the overall increase in accommodation space of the continental Tordillo Formation recorded in the northern Neuquén Basin (Spalletti & Colombo-Piñol, 2005; Spalletti & Veiga, 2007). Furthermore, transgressive lag deposits and/or Glossifungites Ichnofacies were recorded at the base of the Vaca Muerta Formation in other areas (Boll & Valencio, 1996; Borbolla et al., 2014). The rate of coastline migration for the whole Neuquén Basin is far from being resolved because time resolution provided by biostratigraphy based on ammonites is too low to establish the specific timing of the transgression. Therefore, there is a need for these analyses conducted in basinal positions, which might provide a framework to understand how the transgression started and evolved.

CONCLUSIONS

The Kimmeridgian continental deposits of the Quebrada del Sapo Formation represent fluvial, lacustrine and aeolian facies. Jurassic deformation generated an irregular topography prior to flooding. The growth of the Picún Leufú anticline controlled the development of the continental facies of the Quebrada del Sapo Formation and the sedimentary environments of the basal transgressive systems tract (TST) of the Vaca Muerta Formation (both of them thinning towards the anticline). Within the Picún Leufú domain (PL; sections 2, 3 and 4), a planated aeolian–marine contact is present, whereas in the Quebrada del Sapo (QdS; sections 5 to 10) and PL

section 1, a reworked dune-field relief characterized by megadunes is preserved, as indicated by a planation or erosive surface at outcrop-scale and slight thickness changes of strata at large scale. The Vaca Muerta transgression smoothed the pre-flooding relief and a succession accumulated, which is thinner in the topographically high PL domain than in the topographically low QdS domain.

The transgression constituted a rapid, low-energy period representing the transition between the aeolian deposits of the Quebrada del Sapo Formation and the marine basinal facies of the Vaca Muerta Formation. The evolution of the transgression can be subdivided into:

1 Onset of the TST, where rising sea level induced a rising groundwater table that generated a negative sediment budget and facilitated liquefaction and early stabilization of the Quebrada del Sapo aeolian deposits.

2 Beach sediments (F1) accumulated above a sharp to erosive maximum regressive surface due to damp conditions and episodic marine flooding.

3 Early Tithonian extension induced faulting of the beach and aeolian deposits underneath.

4 An embayed coastline developed and microbial mats established (F2).

5 A low-energy, proximal bay with evidence of condensation and winnowing formed above fair-weather wave base (F3).

6 A distal-bay setting characterized by sandy concentrated density flows and storms developed under brackish-water conditions (F4).

7 Distal siliciclastic basin hemipelagic sedimentation established, recording deposition under oxygen-deficient conditions (F5) and showing the maximum flooding surface at the top.

Because a transitional marginal-marine facies association is fairly well-developed, a rapid transgression of the Vaca Muerta Formation is postulated in contrast to previous hypotheses favouring a catastrophic flooding of the aeolian succession. Modern and ancient studies of aeolian to marine transitions suggest three types of transgressions that can be distinguished with respect to timing: (i) catastrophic – abrupt filling of basins after sill or dam break; (ii) rapid – fast sea-level rise events as the Holocene flooding after the Last Glacial Maximum; and (iii) gradual – expressed by stacked parasequences documenting punctuated shoreline migration and producing interbedded aeolian and marine deposits. Modern estuarine sedimentation rates suggest that the embayment succession may have accumulated in a time span of 104 to 105 yr, supporting the rapid transgression hypothesis. At such high rates of sea-level rise, aeolian deposits flooded during low-energy transgressions may record a thin marginal-marine succession with the aeolian landscape preserved below. For the Vaca Muerta Formation, however, the eustatic contribution to relative sea-level rise was relatively small, as indicated by the global eustatic sea-level chart and, therefore, thermal and tectonic subsidence played a major role.

ACKNOWLEDGEMENTS

We thank to Martin Parada, Claudio García, Camila García, Debora Campetella, and the Painemilla family, who offered exceptional support in the Picún Leufú village during field work. We also thank M. Cevallos (CGC), who shared his ideas and provided enormous feedback to the manuscript, and H. Leanza (Universidad Nacional de La Plata), who helped in the determination of bivalves. Valuable comments by Sedimentology reviewers A. Argüello Scotti and J.P. Rodriguez-López, and Associate Editor G.D. Veiga significantly improved the manuscript. This work was financially supported by the Natural Sciences and Engineering

Research Council of Canada (NSERC) Discovery Grants 311727-20, PI-UNRN 2016 40-A-468 and PUE 0031CO to JJP, PI-UNRN 2017 40-A-616 and PIP CONICET 2017 11220170100129CO to NBC, 2016 Student Research Grant from Society for Sedimentary Geology (SEPM), 2016 and 2018 Research Grants from the Geological Society of America (GSA), and 2016 Grants-in-Aid Program of the American Association of Petroleum Geologists (AAPG), and 2018 International Association of Sedimentologists (IAS) post-graduate grant. Field work of AW was financially supported by the Swiss National Fund (grant 200021-169042/1). EP thanks to FINEP, CNPq and FAPERJ to support the Laboratório de Estratigrafia Química e Geoquímica Orgânica (LGQM).

REFERENCES

Abril, J.M. and **Periáñez, R.** (2016) Revisiting the time scale and size of the Zanclean flood of the Mediterranean (5.33 Ma) from CFD simulations. *Marine Geology*, **382**, 242–256.

Acevedo, H. and **Bande, A.** (2018) Characterization of lower Vaca Muerta at Fortín de Piedra in Neuquén Basin, Argentina. *Leading Edge*, **37**, 255–260.

Ahlbrandt, T.S. and **Fryberger, S.G.** (1981) Sedimentary features and significance of interdune deposits. In: *Recent and Ancient Nonmarine Depositional Environments: Models for Exploration* (Eds. F.G. Ethridge and R.M. Flores), *SEPM Special Publication* 31, 293-314.

Ahmed Benan, C.A. and **Kocurek, G.** (2000) Catastrophic flooding of an aeolian dune field: Jurassic Entrada and Todilto formations, Ghost Ranch, New Mexico, USA. *Sedimentology*, **47**, 1069–1080.

Al-Hinai, K.G., **Moore, J.M.** and **Bush, P.R.** (1987) LANDSAT image enhancement study of possible submerged sand-dunes in the Arabian Gulf. *International Journal of Remote Sensing*, **8**, 251–258.

Allmon, W.D. (1988) Ecology of Recent turritelline gastropods (Prosobranchia, Turritellidae): Current knowledge and paleontological implications. *Palaios*, **3**, 259.

Argüello Scotti, A. and **Veiga, G.D.** (2015) Morphological characterization of an exceptionally preserved eolian system: The Cretaceous Troncoso Inferior Member in the Neuquén Basin (Argentina). *Latin American Journal of Sedimentology and Basin Analysis*, **22**, 29–46.

Arregui, C., **Carbone, O.** and **Leanza, H.A.** (2011) Contexto tectosedimentario. In: *Relatorio del XVIII Congreso Geológico Argentino* (Ed. H.A. Leanza, C. Arregui, O. Carbone, J.C. Danieli, and J.M. Vallés), 29–36.

Belknap, D.F. and **Kraft, J.C.** (1981) Preservation potential of transgressive coastal lithosomes on the U.S. Atlantic shelf. *Marine Geology*, **42**, 429–442.

Bentley, S.J. and **Nittrouer, C.A.** (1999) Physical and biological influences on the formation of sedimentary fabric in an oxygen-restricted depositional environment; Eckernförde Bay, southwestern Baltic Sea. *Palaios*, **14**, 585–600.

Blakey, R.C., Peterson, F., Caputo, M.V., Geesaman, R.C. and **Voorhees, B.J.** (1983) Paleogeography of Middle Jurassic continental, shoreline and shallow marine sedimentation, Southern Utah. In: *Mesozoic Paleogeography of West-Central United States* (Eds. M.W. Reynolds and E.D. Dolly), 77-100.

Blakey, R.C., **Havholm, K.G.** and **Jones, L.S.** (1996) Stratigraphic analysis of eolian interactions with marine and fluvial deposits, Middle Jurassic Page Sandstone and Carmel Formation, Colorado Plateau, U.S.A. *Journal of Sedimentary Research*, **66**, 324–342.

Blanc, P.-L. (2002) The opening of the Plio-Quaternary Gibraltar Strait : assessing the size of a cataclysm. *Geodinamica Acta*, **15**, 303–317.

Blaszczyk, J.K. (1981) Palaeomorphology of Weissliegendes top as the control on facies variability in ore-bearing series of Lubin copper-field, Southwestern Poland. *Geologia Sudetica*, **16**, 195–217.

Boll, A. and **Valencio, D.** (1996) Relación estratigráfica entre las formaciones Tordillo y Vaca Muerta en el sector central de la Dorsal de Huincul, Provincia del Neuquén. In: *13º Congreso Geológico Argentino y 3º Congreso de Exploración de Hidrocarburos*, 205–223.

Borbolla, M.C., **Cruz, C.E.**, **Villar, H.J.**, **Annizzotto, N.**, **D'Odorico Benites, P.** and **Cattaneo, D.** (2014) Formación Vaca Muerta: variación lateral de facies y su implicancia en los cambios de espesor hacia el borde se cuenca. Perspectivas exploratorias en shale oil en la Plataforma de Catriel, Cuenca Neuquina, Argentina. In: *IX Congreso de Exploracion y Desarrollo de Hidrocarburos*, 315–339.

Bromley, R.G. and **Uchman, A.** (2003) Trace fossils from the Lower and Middle Jurassic marginal marine deposits of the Sorthat Formation, Bornholm, Denmark. *Bulletin of the Geological Society of Denmark*, **50**, 185–208.

Buatois, L.A. and **Mángano, M.G.** (2011). *Ichnology Organism-Substrate Interactions in Space and Time*. Cambridge University Press, New York, 358 pp.

Buatois, L.A., **Gingras, M.K.**, **MacEachern, J.A.**, **Mángano, M.G.**, **Zonneveld, J.-P.**, **Netto, R.G.** and **Martin, A.** (2005) Colonization of brackish-water systems through time: Evidence from the trace-fossil record. *Palaios*, **20**, 321–347.

Carbone, O., Franzese, J., Limeres, M., Delpino, D. and **Martínez, R.** (2011). El Ciclo Precuyano (Triásico Tardío-Jurásico Temprano) en la Cuenca Neuquina. In: *Relatorio Del XVIII Congreso Geológico Argentino* (Eds. H.A. Leanza *et al.*), pp. 63–76.

Carmona, N., **Bornoud, C.**, **Ponce, J.J.** and **Cuadrado, D.G.** (2011) The role of microbial mats in the preservation of bird footprints: a case study from the mesotidal Bahia Blanca Estuary (Argentina. In: *Microbial Mats in Siliciclastic Depositional Systems Through Time* (Ed. N. Noffke and H. Chafetz), *SEPM Special Publication*, 37–45.

Carmona, N.B., **Ponce, J.J.**, **Wetzel, A.**, **Bournod, C.N.** and **Cuadrado, D.G.** (2012) Microbially induced sedimentary structures in Neogene tidal flats from Argentina: Paleoenvironmental, stratigraphic and taphonomic implications. *Palaeogeography, Palaeoclimatology, Palaeoecology*, **353**–**355**, 1–9.

Cattaneo, A. and **Steel, R.J.** (2003) Transgressive deposits: A review of their variability. *Earth-Science Reviews*, **62**, 187–228.

Catuneanu, O. (2006) *Principles of Sequence Stratigraphy*. Elsevier, 375 pp.

Cevallos, M. (2005) Análisis estratigráfico de alta frecuencia del límite kimmeridgiano-tithoniano en el subsuelo de la Dorsal de Huincul, Cuenca Neuquina. In: *VI Congreso de Exploración y Desarrollo de Hidrocarburos*, Mar del Plata, Actas CD.

Chan, M. and **Kocurek, G.** (1988) Complexities in eolian and marine interactions; processes and eustatic controls on erg development (in Late Paleozoic and Mesozoic eolian deposits of the Western Interior of the United States, Kocurek). *Sedimentary Geology*, **56**, 283–300.

Collinson, J.C. (1994) Sedimentary deformational structures. In: *The Geological Deformation of Sediments* (Ed. A. Maltman), *Chapman and Hall*, London, p. 95–125.

Cornée, J.-J., **Münch, P.**, **Achalhi, M.**, **Merzeraud, G.**, **Azdimousa, A.**, **Quillévéré, F.**, **Melinte-Dobrinescu, M.**, **Chaix, C.**, **Moussa, A. Ben**, **Lofi, J.**, **Séranne, M.** and **Moissette, P.** (2016) The Messinian erosional surface and early Pliocene reflooding in the Alboran Sea: New insights from the Boudinar basin, Morocco. *Sedimentary Geology*, **333**, 115–129.

Damborenea, S.E. and **Leanza, H.A.** (2016). *Huncalotis*, an enigmatic new pectinoid genus (Bivalvia, Late Jurassic) from South America. *Paläontologische Zeitschrift*, 90, 449–468.

De, C. (2000) Neoichnological activities of endobenthic invertebrates in Downdrift Coastal Ganges Delta Complex, India: Their significance in trace fossil interpretations and Paleoshoreline reconstructions. *Ichnos*, **7**, 89–113.

De, C. (2019) *Mangrove Ichnology of the Bay of Bengal Coast, Eastern India*. Springer, 347 pp.

Desmond, R.J., **Steidtmann, J.R.** and **Cardinal, D.F.** (1984) Stratigraphy and depositional environments of the middle member of the Minnelusa Formation, central Powder River Basin, Wyoming. In: *Wyoming Geological Association 35th Annual Field Conference Guidebook*, 213–239.

Díez-Canseco, D., **Buatois, L.A.**, **Mángano, M.G.**, **Rodriguez, W.** and **Solorzano, E.** (2015) The ichnology of the fluvial-tidal transition: Interplay of ecologic and evolutionary controls. In: *Fluvial-Tidal Sedimentology* (Ed. P.J. Ashworth, J.L. Best, and D.R. Parsons), *Developments in Sedimentology*, **68**, 283–321.

Digregorio, J.H. (1972). Neuquén. In: *Geología Regional Argentina* (Ed. A.F. Leanza), 439-505. Academia Nacional de Ciencias, Córdoba.

Doe, T.W. and **Dott, R.H.J.** (1980) Genetic significance of deformed cross bedding–with examples from the Navajo and Weber Sandstones of Utah. *Journal of Sedimentary Petrology*, **50**, 793–812.

Eschner, T.B. and **Kocurek, G.** (1986) Marine destruction of eolian sand seas: Origin of mass-flows. *Journal of Sedimentary Petrology, **56**,* 401–411.

Eschner, T.B. and **Kocurek, G.** (1988) Origins of relief along contacts between eolian sandstones and overlying marine strata. *American Assocation of Petroleum Geologists Bulletin*, **72**, 932–943.

Freije, H., Azúa, G., González, R., Ponce, J.J. and **Zavala, C.A.** (2002). Actividad tectónica sinsedimentaria en el Jurásico del sur de la Cuenca Neuquina. In: *V Congreso de Exploración y Desarrollo de Hidrocarburos*, p. 17. Mar del Plata, Argentina.

Fryberger, S.G. (1984) The Permian Upper Minnelusa Formation, Wyoming: ancient example of an offshore-prograding eolian sand sea with geomorphic facies, and system-boundary traps for petroleum. In: *Wyoming Geological Association 35th Annual Field Conference Guidebook*, 241–271.

Fryberger, S.G. (1986) Stratigraphic traps for petroleum in wind-laid rocks. *American Assocation of Petroleum Geologists Bulletin*, **70**, 1765–1798.

Fryberger, S.G., **Schenk, C.J.** and **Krystinik, L.F.** (1988) Stokes surfaces and the effects of near-surface ground-water-table on eolian deposition. *Sedimentology*, **35**, 21–41.

Fryberger, S.G., **Krystinik, L.F.** and **Schenk, C.J.** (1990) Tidally flooded back-barrier dunefield, Guerrero Negro area, Baja California, Mexico. *Sedimentology*, **37**, 23–43.

Gabbott, S.E., **Zalasiewicz, J.**, **Aldridge, R.J.** and **Theron, J.N.** (2010) Eolian input into the Late Ordovician postglacial Soom Shale, South Africa. *Geology*, **38**, 1103–1106.

Garcia-Castellanos, D., **Estrada, F.**, **Jiménez-Munt, I.**, **Gorini, C.**, **Fernàndez, M.**, **Vergés, J.** and **De Vicente, R.** (2009) Catastrophic flood of the Mediterranean after the Messinian salinity crisis. *Nature*, **462**, 778–781.

Ghinassi, M. (2007) The effects of differential subsidence and coastal topography on high-order transgressive-regressive cycles: Pliocene nearshore deposits of the Val d'Orcia Basin, Northern Apennines, Italy. *Sedimentary Geology*, **202**, 677–701.

Glennie, K.W. and **Buller, A.T.** (1983). The Permian Weissliegend of NW Europe: The partial deformation of aeolian dune sands caused by the Zechstein transgression. *Sedimentary Geology*, **35**, 43–81.

Gründel, J. and **Parent, H.** (2001) Lower and Middle Tithonian marine gastropods from the Neuquén-Mendoza Basin, Argentina. *Bolletino del Instituto de Fisiographía y Geología*, **71**, 13–18.

Gründel, J. and **Parent, H.** (2006) Marine Jurassic gastropods of Argentina. III. Lower and Middle Tithonian of Picún Leufú and Cerro Lotena. *Neues Jahrbuch für Geologie und Paläontologie Monatshefte*, **2006**, 503–512.

Gulisano, C. (1981). El ciclo Cuyano en el norte de Neuquén y sur de Mendoza. In: *8º Congreso Geológico Argentino*, *Actas 3*, pp. 579-592. San Luis, Argentina.

Haq, B.U. (2018) Jurassic Sea-Level Variations: A Reappraisal. *GSA Today*, **28**, 4–10.

Hanebuth, T., **Stattegger, K.** and **Grootes, P.M.** (2000) Rapid flooding of the Sunda Shelf: A Late-Glacial sea-level record. *Science*, **288**, 1033–1035.

Hanebuth, T.J.J., **Stattegger, K.** and **Bojanowski, A.** (2009) Termination of the Last Glacial Maximum sea-level lowstand: The Sunda-Shelf data revisited. *Global and Planetary Change*, **66**, 76–84.

Hanebuth, T.J.J., **Mersmeyer, H.**, **Kudrass, H.R.** and **Westphal, H.** (2013) Aeolian to shallow-marine shelf architecture off a major desert since the Late Pleistocene (northern Mauritania). *Geomorphology*, **203**, 132–147.

Harris, P.T. and **Macmillan-Lawler, M.** (2016) Seafloor mapping along continental shelves. In: *Seafloor Mapping along Continental Shelves: Research and Techniques for Visualizing Benthic Environments* (Ed. C.W. Finkl and C. Makowski), *Springer International Publishing*, Cham, 13, 69–104.

Havholm, K.G. and **Kocurek, G.** (1994) Factors controlling aeolian sequence stratigraphy: clues from super bounding surface features in the Middle Jurassic Page Sandstone. *Sedimentology*, **41**, 913–934.

Howell, J.A., **Schwarz, E.**, **Spalletti, L.A.** and **Veiga, G.D.** (2005) The Neuquén Basin: an overview. In: *The Neuquén Basin, Argentina: A Case Study in Sequence Stratigraphy and Basin Dynamics*

(Ed. G.D. Veiga, L.A. Spalletti, J.A. Howell, and E. Schwarz), *Geological Society of London, Special Publication*, **252**, 1–14.

Hummel, G. and **Kocurek, G.** (1984) Interdune areas of the back-island dune field, north Padre Island, Texas. *Sedimentary Geology*, **39**, 1-26.

Huntoon, J.E. and **Chan, M.A.** (1987) Marine origin of paleotopographic relief on eolian White Rim Sandstone (Permian), Elaterite Basin, Utah. *American Association of Petroleum Geologists Bulletin*, **71**, 1035–1045.

Immenhauser, A. (2005) High-rate sea-level change during the Mesozoic: New approaches to an old problem. *Sedimentary Geology*, **175**, 277–296.

Inman D.L., Ewing, G.C. and **Corliss, J.B.** (1966). Coastal sand dunes of Guerrero Negro, Baja California, Mexico. *Geological Society of America Bulletin,* **77**, 787–802.

Jennings, J.N. (1975) Desert dunes and estuarine fill in the Fitzroy estuary (North-Western Australia). *Catena*, **2**, 215–262.

Joeckel, R.M. and **Korus, J.T.** (2012) Bayhead delta interpretation of an upper Pennsylvanian sheetlike sandbody the broader understanding of transgressive deposits in cyclothems. *Sedimentary Geology*, **274–275**, 22–37.

Jordan, O.D. and **Mountney, N.P.** (2010) Styles of interaction between aeolian, fluvial and shallow marine environments in the Pennsylvanian to Permian lower Cutler beds, south-east Utah, USA. *Sedimentology*, **57**, 1357–1385.

Jordan, O.D. and **Mountney, N.P.** (2012) Sequence stratigraphic evolution and cyclicity of an ancient coastal desert system: The Pennsylvanian-Permian Lower Cutler Beds, Paradox Basin, Utah, U.S.A. *Journal of Sedimentary Research*, **82**, 755–780.

Kaplin, P.A. and **Selivanov, A.O.** (2004) Late-glacial and Holocene sea level changes in semi-enclosed seas of North Eurasia: Examples from the contrasting Black and White Seas. *Palaeogeography, Palaeoclimatology, Palaeoecology*, **209**, 19–36.

Kidwell, S.M. and **Aigner, T.** (1985). Sedimentary dynamics of complex shell beds: Implications for ecologic and evolutionary patterns. In: *Sedimentary and Evolutionary Cycles* (Eds. U. Bayer, A. Seilacher), pp. 382–395.

Kietzmann, D.A., **Iglesia Llanos, M.P.**, **Ivanova, D.K.**, **Kohan Martínez, M.** and **Sturlesi, M.A.** (2018) Toward a multidisciplinary chronostratigraphic calibration of the Jurassic-Cretaceous transition in the Neuquén Basin. *Revista de la Asociación Geológica Argentina,* **75**, 175–187.

Knaust, D. (2018) The ichnogenus *Teichichnus* Seilacher, 1955. *Earth-Science Reviews*, **177**, 386–403.

Kocurek, G. (1981) Significance of interdune deposits and bounding surfaces in aeolian dune sands. *Sedimentology*, **28**, 753–780.

Kocurek, G. and **Nielson, J.** (1986) Conditions favourable for the formation of warm-climate aeolian sand sheets. *Sedimentology*, **33**, 795–816.

Kocurek, G., **Robinson, N.I.** and **Sharp, J.M.** (2001) The response of the water table in coastal aeolian systems to changes in sea level. *Sedimentary Geology*, **139**, 1–13.

Kocurek, G., **Martindale, R.C.**, **Day, M.**, **Goudge, T.A.**, **Kerans, C.**, **Hassenruck-Gudipati, H.J.**, **Mason, J.**, **Cardenas, B.T.**, **Petersen, E.I.**, **Mohrig, D.**, **Aylward, D.S.**, **Hughes, C.M.** and **Nazworth, C.M.** (2019) Antecedent aeolian dune topographic control on carbonate and evaporite facies: Middle Jurassic Todilto Member, Wanakah Formation, Ghost Ranch, New Mexico, USA. *Sedimentology*, **66**, 808–837.

Krim, N., **Bonnel, C.**, **Tribovillard, N.**, **Imbert, P.**, **Aubourg, C.**, **Riboulleau, A.**, **Bout-Roumazeilles, V.**, **Hoareau, G.** and **Fasentieux, B.** (2017) Paleoenvironmental evolution of the southern Neuquèn basin (Argentina) during the Tithonian-Berriasian (Vaca Muerta and Picún Leufú Formations): a multi-proxy approach. *Bulletin de la Société géologique de France*, **188**, 34.

Krim, N., **Tribovillard, N.**, **Riboulleau, A.**, **Bout-Roumazeilles, V.**, **Bonnel, C.**, **Imbert, P.**, **Aubourg, C.**, **Hoareau, G.** and **Fasentieux, B.** (2019) Reconstruction of palaeoenvironmental conditions of the Vaca Muerta formation in the southern part of the Neuquén Basin (Tithonian-Valanginian): Evidences of initial short-lived development of anoxia. *Marine and Petroleum Geology*, **103**, 176–201.

Lazar, O.R., **Bohacs, K.M.**, **Macquaker, J.H.S.**, **Schieber, J.** and **Demko, T.M.** (2015) Capturing key attributes of fine-grained sedimentary rocks in outcrops, cores, and thin sections: Nomenclature and description guidelines. *Journal of Sedimentary Research*, **85**, 230–246.

Leanza, H.A. (1973) Estudio sobre los cambios faciales de los estratos limitrofes Jurasico-Cretacicos entre Loncopue y Picun Leufu, provincia de Neuquén, Republica Argentina. *Revista de la Asociación Geológica Argentina*, **28**, 97–132.

Leanza, H.A. and **Hugo, C.A.** (1977). Sucesión de amonites y edad de la Formación Vaca Muerta y sincrónicas entre los paralelos 35° y 40° l.s., Cuenca Neuquina-Mendocina. *Revista de la Asociación Geológica Argentina,* **32**, 248–264.

Leanza, H.A. and **Hugo, C.A.** (1997) Hoja geológica 3969-III, Picún Leufú. Instituto de Geología y Recursos Minerales.

Leanza, H.A., **Sattler, F.**, **Martinez, R.S.** and **Carbone, O.** (2011) La Formación Vaca Muerta y equivalentes (Jurásico Tardío-Cretácico Temprano) en la Cuenca Neuquina. In: *Relatorio del XVIII Congreso Geológico Argentino* (Ed. H.A. Leanza, C. Arregui, O. Carbone, J.C. Danieli, and J.M. Vallés), Buenos Aires, 113–130.

Legarreta, L. (2001). Desiccation events and non-marine clastic lowstands in the Neuquina Basin: Stratigraphy, facies and hydrocarbon distribution. In: *Hedberg Conference, American Association of Petroleum Geologists,* Mendoza, pp. 28–29.

Legarreta, L. (2002). Eventos de desecación en la Cuenca Neuquina: depósitos continentales y distribución de hidrocarburos. In: *5º Congreso de Exploración y Desarrollo de Hidrocarburos*, Mar del Plata.

Legarreta, L. and **Gulisano, C.** (1989). Análisis estratigráfico secuencial de la Cuenca Neuquina (Triásico Superior - Terciario Inferior), Argentina. In: *Cuencas Sedimentarias Argentinas*, (Eds. G.A. Chebli and L.A. Spalletti), *Serie Correlación Geológica*, 6, 221–243.

Lobza, V. and **Schieber, J.** (1999). Biogenic sedimentary structures produced by worms in soupy, soft muds: observations from the Chattanooga Shale (Upper Devonian) and Experiments. *Journal of Sedimentary Research*, **69**, 1041–1049.

MacEachern, J.A. and **Gingras, M.K.** (2007) Recognition of brackish-water trace-fossil suites in the Cretaceous Western Interior Seaway of Alberta, Canada. In: *Sediment-Organism Interactions; A Multifaceted Ichnology* (Ed. R.G. Bromley, L.A. Buatois, G. Mángano, J.F. Genise, and R.N. Melchor), *SEPM Special Publication*, **88**, 149–193.

MacEachern, J. A., Raychaudhuri, I. and **Pemberton, S. G.** (1992). Stratigraphic applications of the *Glossifungites* ichnofacies: delineating discontinuities in the rock record. In: *Applications of Ichnology to Petroleum Exploration* (Ed. S.G. Pemberton), *Society of Economic Paleontologists and Mineralogists Core Workshop Notes*, **17**, 169–198.

MacEachern, J. A., Pemberton, S. G., Bann, K. L. and **Gingras, M. K.** (2007) Departures from the archetypal Ichnofacies: Effective recognition of physico-chemical stresses in the rock record. In: *Applied Ichnology* (Eds. J.A. MacEachern, K.L. Bann, M.K. Gingras, and S.G. Pemberton), *SEMP Short Courses,* **52**, 65–93.

MacEachern, J. A., Dashtgard, S.E., Knaust, D., Catuneanu, O., Bann, K.K. and **Pemberton, S. G.** (2012) Sequence stratigraphy. In: *Trace Fossils as Indicators of Sedimentary Environments* (Ed. D. Knaust and R.G. Bromley), *Developments in Sedimentology,* **64**, 157–195.

Moore, W.R. (1983) The nature of the Minnelusa-Opeche contact in the Halverson field area, Powder River basin, Wyoming. *Mountain Geology*, **20**, 113–120.

Mosquera, A., **Silvestro, J.**, **Ramos, V.A.**, **Alarcón, M.** and **Zubiri, M.** (2011) La estructura de la Dorsal de Huincul. In: *Relatorio del XVIII Congreso Geológico Argentino* (Ed. H.A. Leanza, C. Arregui, O. Carbone, J.C. Danieli, and J.M. Vallés), Buenos Aires, 385–398.

Mpodozis, C. and **Ramos, V.A.** (2008). Tectónica jurásica en Argentina y Chile: extensión, subducción oblicua, rifting, deriva y colisiones? *Revista de la Asociación Geológica Argentina*, **63**, 481–497.

Mutti, E., Gulisano, C.A. and **Legarreta, L.** (1994). Anomalous systems tracts stacking patterns within 3rd. Orden depositional sequences (Jurassic–Cretaceous backarc Neuquén Basin, Argentina Andes. In: *Second High Resolution Sequence Stratigraphy Conference, Abstracts* (Eds. H.W. Posamentier and E. Mutti), pp. 137-143. Tremp.

Naipauer, M., García Morabito, E., Marques, J.C., Tunik, M., Rojas Vera, E.A., Vujovich, G.I., Pimentel, M.P. and **Ramos, V.A.** (2012). Intraplate Late Jurassic deformation and exhumation in western central Argentina: Constraints from surface data and U-Pb detrital zircon ages. *Tectonophysics*, **524–525**, 59–75.

Nichols, M.M. (1989) Sediment accumulation rates and relative sea-level rise in lagoons. *Marine Geology*, **88**, 201–219.

Noffke, N. (2010). *Geobiology: Microbial Mats in Sandy Deposits from the Archaean Era to Today*. Springer, Heidelberg, 194 pp.

Nummedal, D. and **Swift, D.J.P.** (1987) Transgressive stratigraphy at sequence-bounding unconformities: some principles derived from Holocene and Cretaceous examples. In: *Sea-Level Fluctuation and Coastal Evolution* (Ed. D. Nummedal, O.H. Pilkey, and J.D. Howard), *SEPM Special Publication*, **41**, 241–260.

Paola, C., Wiele, S.M. and **Reinhardt, M.A.** (1989). Upper-regime parallel lamination as the result of turbulent sediment transport and low-amplitude bedforms. *Sedimentology*, **36**, 47–59.

Parent, H., Garrido, A.C., Schweigert, G. and **Scherzinger, A.** (2011). The Tithonian ammonite fauna and stratigraphy of Picún Leufú, southern Neuquén Basin, Argentina. *Revue de Paléobiologie Genève* 30, 45–104.

Parker, G. (1965). Relevamiento geológico escala 1:100.00 – Hoja 4169-3, I.G.M. Lonco Vaca. Provincia de Río Negro. YPF unpublished report, Buenos Aires.

Paz, M., **Ponce, J.J.**, **Buatois, L.A.**, **Mángano, M.G.**, **Carmona, N.B.**, **Pereira, E.** and **Desjardins, P.R.** (2019) Bottomset and foreset sedimentary processes in the mixed carbonate-siliciclastic Upper Jurassic-Lower Cretaceous Vaca Muerta Formation, Picún Leufú Area, Argentina. *Sedimentary Geology*, **389**, 161–185.

Pemberton, S.G. and **Frey, R.W.** (1985) The *Glossifungites* Ichnofacies: Modern Examples from the Georgia Coast, U.S.A. In: *Biogenic Structures: Their Use in Interpreting Depositional Environments* (Ed. H.A. Curran), *SEPM (Society for Sedimentary Geology) Special Publication*, **35**, 237–259.

Pemberton, S.G., Spila, M., Pulham, A. J., Saunders, T., MacEachern, J. A., Robbins, D. and **Sinclair, I. K.** (2001) Ichnology and sedimentology of shallow to marginal marine systems. *Geological Association of Canada, Short Course Notes*, **15**, 343 pp.

Petersen, H.I., **Andsbjerg, J.**, **Bojesen-Koefoed, J.A.**, **Nytoft, H.P.** and **Rosenberg, P.** (1998) Petroleum potential and depositional environments of Middle Jurassic coals and non-marine deposits, Danish Central Graben, with special reference to the Søgne Basin. *Geological Survey of Denmark Bulletin*, **36**, 78 pp.

Ponce, J.J., **Carmona, N.**, **Montagna, A.O.** and **Canale, N.** (2015) Sedimentología e Icnología de los sistemas petroleros no Convencionales de la Cuenca Neuquina. *Universidad Nacional de Río Negro - Fundación YPF*, 112 pp.

Ponce, J.J, Carmona, N., Wetzel, A. and **Paz, M.** (2016). Sedimentología e Icnología del tramo basal de la Formación Vaca Muerta, Cuenca Neuquina, Argentina: Implicancias en el análisis de la transgresión del Tithoniano. In: *7° Latin American Congress of Sedimentology and 15th Argentinean Meeting of Sedimentology*, p. 136. Santa Rosa, Argentina

Pye, K. (1983) Early post-depositional modification of aeolian dune sands. In: *Eolian Sediments and Processes, Developments in Sedimentology* (Ed. M.E. Brookfield and T.S. Ahlbrandt), Elsevier, Amsterdam, **38**, 197–221.

Raiswell, R. and **Fisher, Q.J.** (2004) Rates of carbonate cementation associated with sulphate reduction in DSDP/ODP sediments: Implications for the formation of concretions. *Chemical Geology*, **211**, 71–85.

Ramos, V.A. and **Folguera, A.** (2005). Tectonic evolution of the Andes of Neuquén: Constraints derived from the magmatic arc and foreland deformation. In: *The Neuquén Basin, Argentina: A Case Study in Sequence Stratigraphy and Basin Dynamics* (Eds. G.D. Veiga *et al.*), *Geological Society of London*, *Special Publication,* **252**, 15–35.

Reijenstein, H.M., Posamentier, H.W., Fantín, M.A., González Tomassini, F. and **Lipinski, C.** (2014). Vaca Muerta Seismic Stratigraphy and Geomorphology: Regional Architectural Trends for Unconventional Exploration. In: *IX Congreso de Exploración y Desarrollo de Hidrocarburos*, *Abstracts Extendidos*, pp. 211–220. Mendoza, Argentina.

Riccardi, A.C. (2008). El Jurásico de la Argentina y sus amonites. *Revista de la Asociación Geológica Argentina*, **63**, 625–643.

Riccardi, A.C. (2015) Remarks on the Tithonian–Berriasian ammonite biostratigraphy of west central Argentina. *Volumina Jurassica*, **13 (2)**, 23–52.

Rodríguez-López, J.P., **Meléndez, N.**, **de Boer, P.L.** and **Soria, A.R.** (2012) Controls on marine-erg margin cycle variability: Aeolian-marine interaction in the mid-Cretaceous Iberian Desert System, Spain. *Sedimentology*, **59**, 466–501.

Röhl, H.J., Schmidt-Röhl, A., Oschmann, W., Frimmel, A. and **Schwark, L.** (2001) The Posidonia Shale (Lower Toarcian) of SW Germany: An oxygen depleted ecosystem controlled by sea level and paleoclimate. *Palaeogeography, Palaeoclimatology, Palaeoecology*, **165**, 27–52.

Ryan, W. and **Pitman, W.** (1998) *Noah's Flood: The New Scientific Discoveries about the Event that Changed History*. Simon & Schuster, New York, 320 pp.

Ryan, W.B.F., **Pitman, W.C.**, **Major, C.O.**, **Shimkus, K.**, **Moskalenko, V.**, **Jones, G.A.**, **Dimitrov, P.**, **Gorür, N.**, **Sakinç, M.** and **Yüce, H.** (1997) An abrupt drowning of the Black Sea shelf. *Marine Geology*, **138**, 119–126.

Schieber, J. (1986). The possible role of benthic microbial mats during the formation of carbonaceous shales in shallow Mid-Proterozoic basins. *Sedimentology*, **33**, 521–536.

Schieber, J. (2007). Microbial mats on muddy substrates – Examples of possible sedimentary features and underlying processes. In: *Atlas of Microbial Mat Features Preserved within the Siliciclastic Rock Record* (Eds. J. Schieber, P.K. Bose, P.G. Eriksson, S. Banerjee, S. Sarkar, W. Altermann, O. Catuneanu), *Elsevier*, pp. 117–134.

Shinn, E. A. (1973) Sedimentary Accretion along the Leeward, SE Coast of Qatar Peninsula, Persian Gulf. In: *The Persian Gulf* (Ed. B.H. Purser), *Springer-Verlag*, pp. 199–210.

Smith, D.B. (1979) Rapid marine transgressions and regressions of the Upper Permian Zechstein Sea. *Journal of the Geological Society London*, **136**, 155–156.

Spalletti, L.A. and **Colombo Piñol, F.** (2005) From alluvial fan to playa: An Upper Jurassic ephemeral fluvial system, Neuquen Basin, Argentina. *Gondwana Research*, **8**, 363–383.

Spalletti, L.A. and **Veiga, G.D.** (2007) Variability of continental depositional systems during lowstand sedimentation: An example from the Kimmeridgian of the Neuquén Basin, Argentina. *Latin American Journal of Sedimentology and Basin Analysis*, **14**, 85–104.

Spalletti, L.A., **Franzese, J.R.**, **Matheos, S.D.** and **Schwarz, E.** (2000) Sequence stratigraphy of a tidally dominated carbonate-siliciclastic ramp; the Tithonian-Early Berriasian of the Southern Neuquén Basin, Argentina. *Journal of the Geological Society London*, **157**, 433–446.

Steele, R.P. (1983) Longitudinal draa in the Permian Yellow Sands of north-fast England. In: *Eolian Sediments and Processes* (Ed. M.E. Brookfield and T.S. Ahlbrandt), *Developments in Sedimentology,* **38**, 543–550.

Stipanicic, P. N., Rodrigo, F., Baulies, O.L. and **Martínez, C.G.** (1968). Las Formaciones presenonianas en el denominado Macizo Nordpatagónico y regiones adyacentes. *Revista de la Asociación Geológica Argentina*, **23**, 367–388.

Strohmenger, C.J., Al-Mansoori, A., Al-Jeelani, O., Al-Shamry, A., Al-Hosani, I., Al-Mehsin, K. and **Shebl, H.** (2010). The sabkha sequence at Mussafah Channel (Abu Dhabi, United Arab Emirates): Facies stacking patterns, microbial-mediated dolomite and evaporite overprint. *GeoArabia*, **15** (1), 49–90.

Strömbäck, A. and **Howell, J.A.** (2002) Predicting distribution of remobilized aeolian facies using sub-surface data: the Weissliegend of the UK Southern North Sea. *Petroleum Geoscience*, **8**, 237–249.

Strömbäck, A., **Howell, J.A.** and **Veiga, G.D.** (2005) The transgression of an erg – sedimentation and reworking/soft-sediment deformation of aeolian facies: The Cretaceous Troncoso Member, Neuquén Basin, Argentina. In: *The Neuquén Basin, Argentina: A Case Study in Sequence Stratigraphy and Basin Dynamics* (Ed. G.D. Veiga, L.A. Spalletti, J.A. Howell, and E. Schwarz), *Geological Society, London, Special Publications*, **252**, 163–183.

Swift, D.J.P. (1968) Coastal erosion and transgressive stratigraphy. *J. Geol.*, **76**, 444–456.

Szczuciński, W., Jagodziński, R., Hanebuth, T. J. J., Stattegger, K., Wetzel, A., Mitręga, M., Unverricht, D., and **Van Phach, P.** (2013) Modern sedimentation and sediment dispersal pattern on the continental shelf off the Mekong River delta, South China Sea. *Global Planetary Change*, **110**, 195–213.

Tanner, W.F. (1967) Ripple mark indices and their uses. *Sedimentology*, **9**, 89–104.

Tanner, W.F. (1970) Triassic-Jurassic lakes in New Mexico. *Mt. Geol.*, **7**, 281–289.

Taylor, A.M. and **Goldring, R.** (1993). Description and analysis of bioturbation and ichnofabric. *Journal of the Geological Society London*, **150**, 141–148.

Tunik, M., Folguera, A., Naipauer, M., Pimentel, M. and **Ramos, V.A.** (2010). Early uplift and orogenic deformation in the Neuquén Basin: Constraints on the Andean uplift from U-Pb and Hf isotopic data of detrital zircons. *Tectonophysics*, **489**, 258–273.

Uliana, M.A., Legarreta, L., Laffitte, G.A. and **Villar, H.** (1999). Estratigrafía y geoquímica de las facies generadoras de hidrocarburos en las Cuencas Petrolíferas de Argentina. In: *4º Congreso de Exploración y Desarrollo de Hidrocarburos. Trabajos Técnicos. Simposio de Sistemas Petroleros de las Cuencas Argentinas.* CD ROM. Mar del Plata, Argentina.

Van West, F.P. (1972) Trapping mechanism of Minnelusa oil accumulations, Northeastern Powder River basin, Wyoming. *Mountain Geology*, **9**, 3–20.

Veiga, G.D. and **Spalletti, L.A.** (2007). The Upper Jurassic (Kimmeridgian) fluvial-aeolian systems of the southern Neuquén Basin, Argentina. *Gondwana Research*, **11**, 286–302.

Vennari, V. V., **Lescano, M.**, **Naipauer, M.**, **Aguirre-Urreta, M.B.**, **Concheyro, A.**, **Schaltegger, U.**, **Armstrong, R.**, **Pimentel, M.** and **Ramos, V.A.** (2014) New constraints on the Jurassic-Cretaceous boundary in the High Andes using high-precision U-Pb data. *Gondwana Research*, **26**, 374–385.

Vergani, G.D., Tankard, A.J., Belotti, H.J. and **Welsink, H.J.** (1995). Tectonic evolution and paleogeography of the Neuquén Basin, Argentina. In: *Petroleum Basins of South America* (Eds. A.J. Tankard, R. Suarez Soruco and H.J. Welsink), *American Association of Petroleum Geologists Memoirs*, **62,** 383–402.

Vincelette, R.R. and **Chittum, W.E.** (1981) Exploration for oil accumulations in Entrada Sandstone, San Juan Basin, New Mexico. *American Association of Petroleum Geologists Bulletin*, **65**, 2546–2570.

Waite, R. and **Strasser, A.** (2011) A comparison of recent and fossil large, high-spired gastropods and their environments: The Nopparat Thara tidal flat in Krabi, South Thailand, versus the Swiss Kimmeridgian carbonate platform. *Facies*, **57**, 223–248.

Wetzel, A. and **Allia, V.** (2000) The significance of hiatus beds in shallow-water mudstones: An example from the Middle Jurassic of Switzerland. *Journal of Sedimentary Research*, **70**, 170–180.

Wetzel, A. and **Uchman, A.** (1998). Biogenic sedimentary structures in mudstones - an overview. In: *Shales and Mudstones I* (Eds. J. Schieber, W. Zimmerle and P. Sethi), 351–369. Schweizerbart, Stuttgart.

Wetzel, A., **Szczygielski, A.**, **Unverricht, D.** and **Stattegger, K.** (2017) Sedimentological and ichnological implications of rapid Holocene flooding of a gently sloping mud-dominated incised valley – an example from the Red River (Gulf of Tonkin). *Sedimentology*, **64**, 1173–1202.

Yanko-Hombach, V., **Gilbert, A.S.**, **Panin, N.** and **Dolukhanov, P.M.** (2007) The Black Sea flood question: Changes in coastline, climate and human settlement. *Springer*, Dordrecht, The Netherlands, 971 pp.

Yokoyama, Y., **De Deckker, P.**, **Lambeck, K.**, **Johnston, P.** and **Fifield, L.** (2001) Sea-level at the Last Glacial Maximum: evidence from northwestern Australia to constrain ice volumes for oxygen isotope stage 2. *Palaeogeography, Palaeoclimatology, Palaeoecology*, **165**, 281–297.

Zanettini, J.C.M. (1979). Geología de la comarca de Campana Mahuida (Provincia del Neuquén). *Revista de la Asociación Geológica Argentina*, **34**, 61-68.

Zavala, C.A. and **Freije, H.** (2002). Cuñas clásticas jurásicas vinculadas a la Dorsal de Huíncul. Un ejemplo del area de Picun Leufu. Cuenca Neuquina, Argentina. In: *V Congreso de Exploración y Desarrollo de Hidrocarburos*, pp. 14. Mar del Plata, Argentina.

Zavala, C.A., Maretto, H. and **Di Meglio, M.** (2005). Hierarchy of bounding surfaces in aeolian sandstones of the Jurassic Tordillo Formation (Neuquén Basin, Argentina). *Geologica Acta*, 3, 133–145.

Zavala, C.A., Lampe, J.M.M., Fernández, M., Di Meglio, M. and **Arcuri, M.** (2008). El diacronismo entre las formaciones Tordillo y Quebrada del Sapo (Kimeridgiano) en el sector sur de la cuenca Neuquina. *Revista de la Asociación Geológica Argentina*, **63**, 754–765.

Zeller, M. (2013). Facies, Geometries and Sequence Stratigraphy of the Mixed Carbonate - Siliciclastic Quintuco - Vaca Muerta System in the Neuquén Basin, Argentina: An Integrated Approach. Open Access Diss. Thesis, University of Miami, 206 pp.

Zeller, M., **Verwer, K.**, **Eberli, G.P.**, **Massaferro, J.L.**, **Schwarz, E.** and **Spalletti, L.A.** (2015) Depositional controls on mixed carbonate-siliciclastic cycles and sequences on gently inclined shelf profiles. *Sedimentology*, **62**, 2009–2037.

Supporting Information for Paz *et al.*

Stratigraphic sections of the study area. See Figure 1 and 3 for location of the sections. Next to the sections is the facies (F) and facies association (FA) interpretation.

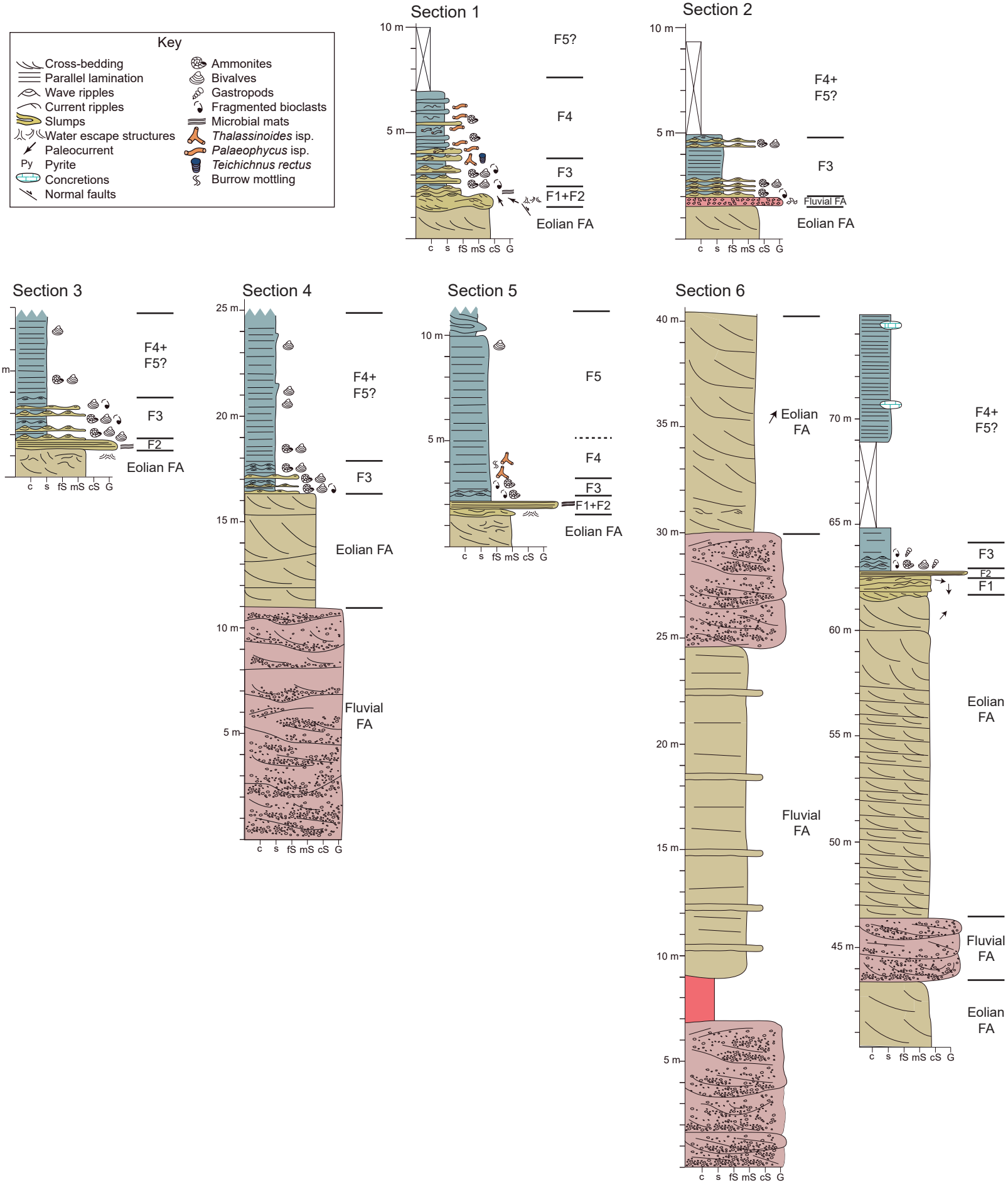

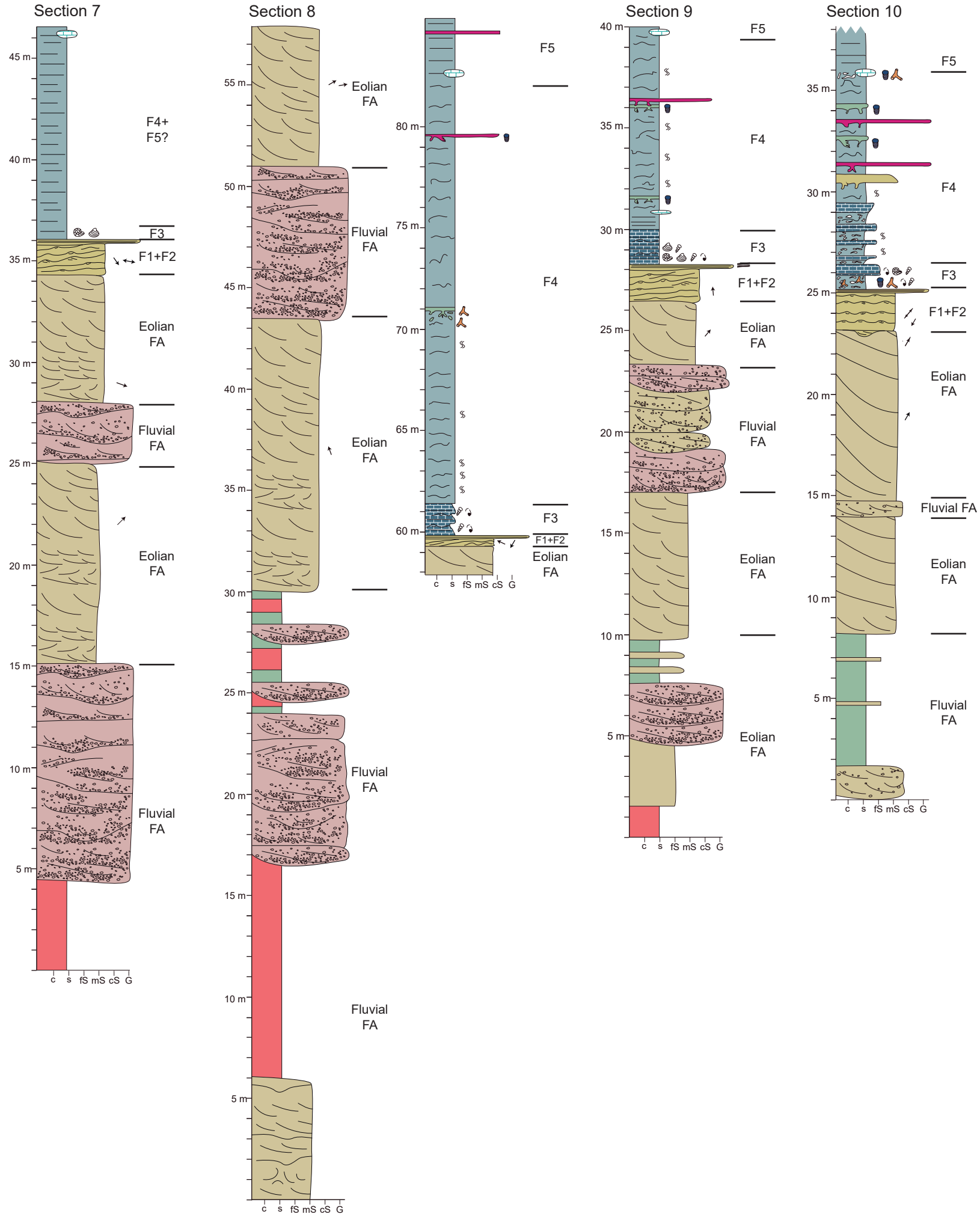
Section 7
45 m
40 m
35 m
30 m
25 m
20 m
15 m
10 m
5 m
F4+
F5?
F3
F1+F2
Eolian
FA
Fluvial
FA
Eolian
FA
Eolian
FA
Fluvial
FA
c s fS mS cS G
Section 8
55 m
50 m
45 m
40 m
35 m
30 m
25 m
20 m
15 m
10 m
5 m
Eolian
FA
Fluvial
FA
Eolian
FA
Fluvial
FA
Fluvial
FA
c s fS mS cS G
80 m
75 m
70 m
65 m
60 m
F5
F4
F3
F1+F2
Eolian
FA
c s fS mS cS G
Section 9
40 m
35 m
30 m
25 m
20 m
15 m
10 m
5 m
F5
F4
F3
F1+F2
Eolian
FA
Fluvial
FA
Eolian
FA
Eolian
FA
c s fS mS cS G
Section 10
35 m
30 m
25 m
20 m
15 m
10 m
5 m
F5
F4
F3
F1+F2
Eolian
FA
Fluvial FA
Eolian
FA
Fluvial
FA
c s fS mS cS G